Science Journal of Chemistry
2023; 11(3): 88-107
http://www.sciencepublishinggroup.com/j/sjc
doi: 10.11648/j.sjc.20231103.13
ISSN: 2330-0981 (Print); ISSN: 2330-099X (Online)

Modelling Interactions Between Flavanols and Amine Acids: Case of Catechin and Epicatechin with Alanine; NBO, AIM, NCI Analysis

Essoh Akpa Eugene[1], N'Guessan Boka Robert[1], Adenidji Ganiyou[2], Adjou Ane[1], Bamba El Hadji Sawaliho[1, *]

[1]Laboratory of Constitution and Reaction of Matter, Training and Research Unit in Structural Sciences, Materials and Technology, Felix Houphouet-Boigny University, Abidjan, Ivory Coast

[2]Laboratory of Environmental Sciences and Technologies, Training and Research Unit in Environment, Jean Lorougnon Guede University, Daloa, Ivory Coast

Email address:

essohakpaeugene@gmail.com (Essoh Akpa Eugene), nguessanbr@yahoo.fr (N'Guessan Boka Robert), adjouane@hotmail.com (Adjou Ane), adeganiyou@gmail.com (Adenidji Ganiyou), bambaelhadjisawaliho@yahoo.ca (Bamba El Hadji Sawaliho)

[*]Corresponding author

To cite this article:

Essoh Akpa Eugene, N'Guessan Boka Robert, Adenidji Ganiyou, Adjou Ane, Bamba El Hadji Sawaliho. Modelling Interactions Between Flavanols and Amine Acids: Case of Catechin and Epicatechin with Alanine; NBO, AIM, NCI Analysis. *Science Journal of Chemistry.* Vol. 11, No. 3, 2023, pp. 88-107. doi: 10.11648/j.sjc.20231103.13

Received: May 10, 2023; **Accepted**: May 29, 2023; **Published**: June 9, 2023

Abstract: The interactions between two flavanols (Catechin and Epicatechin) and (Ala) Alanine (aliphatic amino acid) are evaluated by theoretical chemistry methods. Calculations at the level DFT/B3LYP/6-31+G (d, p) determine their characteristics and those of the monomers. Geometric, energetic, and spectroscopic parameters in addition to QTAIM (Quantum Theory of Atoms In Molecules), NBO (Natural Bond Orbital) and NCI (Non-Covalent Interaction) topological analyses qualify the nature and type of these. The results indicate that the main interactions are O–H···O and O–H···N between the hydroxyl groups of Cat (Catechin) or Epicat (Epicatechin) and the heteroatoms of Ala. They mention the existence of a secondary one alongside the main. They classify them into proper, improper, moderate, and weak. The spectroscopic parameters prove that O–H···O, O–H···N and N–H···O are proper. They establish that the C–H···N and C–H···O are improper. QTAIM analysis presents O–H···O, O–H···N interactions as moderate and C–H···O and N–H···O as weak. Stabilization energies show that the most reactive sites of Ala N_{sp^3} and O_{sp^2} interact strongly with the O_{28}–H_{29}, O_{32}–H_{33} and O_{34}–H_{35} hydroxyl groups of EpiCat and Cat. These interactions lead to the most stable complexes. This research reveals the existence of the VDW (Van Der Walls) NCI type and repulsive (steric) interactions in these complexes.

Keywords: Flavanols, Catechin, Epicatechin, NBO, AIM, NCI, Hydrogen Bond

1. Introduction

Polyphenols are organic compounds well known to interact with organic and inorganic compounds. They are found in the vegetation kingdom. They are metabolized by plants to fight against all kinds of external aggression [1, 2]. Humans consume them primarily for their many antioxidants or anti-inflammatory properties [3–8]. It is also used to prevent and treat neurodegenerative diseases [9, 10]. Polyphenols are grouped into classes; these include phenolic acids, hydroxy-cinnamic acids, phenylacetic acids, aceto-phenols, coumarin, xantones, stilbenes and flavonoids [11, 12]. Each is made up of several subfamilies. So, flavonoids contain that of flavanols.

When eating certain foods (fruits, vegetables, wine, and tea), polyphenols are released into the body. These encounter its compounds. They generate interactions. Indeed, a lot of theoretical and experimental research establish their existences between polyphenols and organic or inorganic molecules. Proteins, lipids, or sugars represent the first. Iron and magnesium are some examples of the second [13–17]. These interactions generally take place with the hydroxyl

groups of the polyphenols [18]. The theoretical study of Cat (Catechin) and EpiCat (Epicatechin) proves that the most reactive sites are the latter [19].

Moreover, many authors attest that the interactions of polyphenols with proteins are usually non-covalent, including those with HB (Hydrogen Bonds) [20–22]. These are important in biological processes; they influence the properties of water as a universal natural solvent [23]. They also contribute determining the structure and characteristics of several biotic molecules such as proteins [24]. However, in some cases, irreversible interactions may occur [25]. These interactions, both covalent and non-covalent, can modify those of polyphenols and proteins. This asset can justify the supposed virtues of polyphenols; these help to fight against certain illnesses. Polyphenols can reduce or prevent the appearance of many mechanisms involved in the genesis or in the cardiovascular or cancerous disease amplification [10, 26]. They associate with the proteins underlying these diseases. Nevertheless, few studies offer quantitative information that facilitates categorizing polyphenol-protein interactions. This research targets identifying and classifying those between two flavan-3-ols and an amino acid.

The first compounds correspond to a subclass of polyphenols. The second constitutes a basic component of proteins. In addition, this work aims to understand the stability of complexes correlated with their reactions. This would provide a more comprehensive database for the study of polyphenol-protein associations. Cat and EpiCat are the two flavan-3-ols used because of their high abundance in the human diet; Ala represents the amino acid [27, 28]. This will give us insight into the interactions of these two flavanols with the latter.

This research optimizes the geometry of the chemical structures studied. A frequency calculation performed in the gas phase follows this operation. Both estimates are made with the DFT method at the theoretical level B3LYP 6–31 G+ (d, p). These calculations concern the monomers Cat, EpiCat and Ala. They also relate to the Cat-Ala and EpiCat-Ala complexes. They lead to their geometric, energetic, and vibratory parameters.

In addition, a NBO (Natural Bond Orbital) analysis was achieved on the complexes under study. It makes it possible to examine CT (LP transfers) and hybridization states during the interactions. A QTAIM investigation was carried out; It helps to identify their strength and the stability of complexes. Finally, this work implements a NCI (Non-Covalent Interaction) scrutiny. It aims to clarify their nature within these chemical structures.

2. Material and Computational Methods

2.1. Calculation Methods

The GAUSSIAN 09 software was used to optimize the geometries of the molecules [29, 30]. Figure 1 shows the structures obtained from Cat, Epicatechin (Epicat) or Alanine (Ala). Those of the Cat… Ala and EpiCat… Ala (Epicat… Ala) complexes appear respectively in figures 2 and 3. These complexes result from the interactions between the hydroxyls groups of the Cat or EpiCat and Ala heteroatoms. The first reactants designate O_{28}- H_{29}, O_{32}- H_{33}, O_{34}- H_{35}. The second ones refer to Nsp^3, Osp^3 and Osp^2 [19]. The AIMALL software exploits the" formatted checkpoint file" of geometrical optimizations for topological exams of electron density [31]. The NBO analysis is carried out based on a "single point" calculation from these structures obtained [30, 32]. Multiwfn and Chemcraft software were used to perform respectively the NCI assessment and the surface representation of this latter [33, 34].

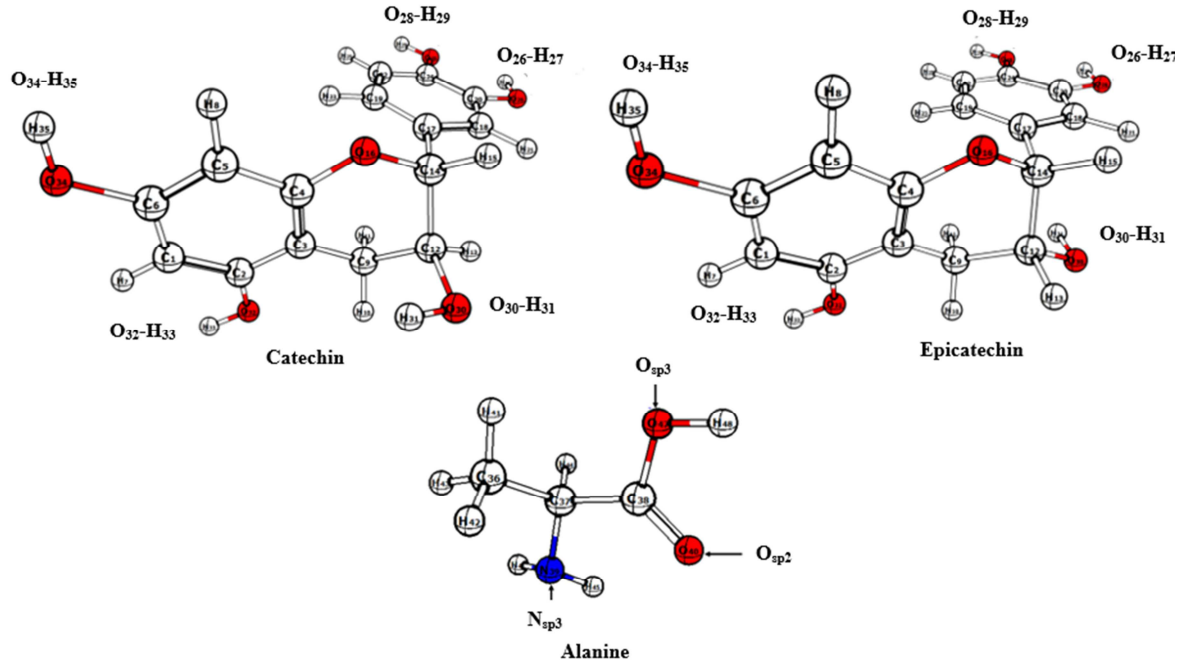

Figure 1. *Structures of Cat, EpiCat and Ala.*

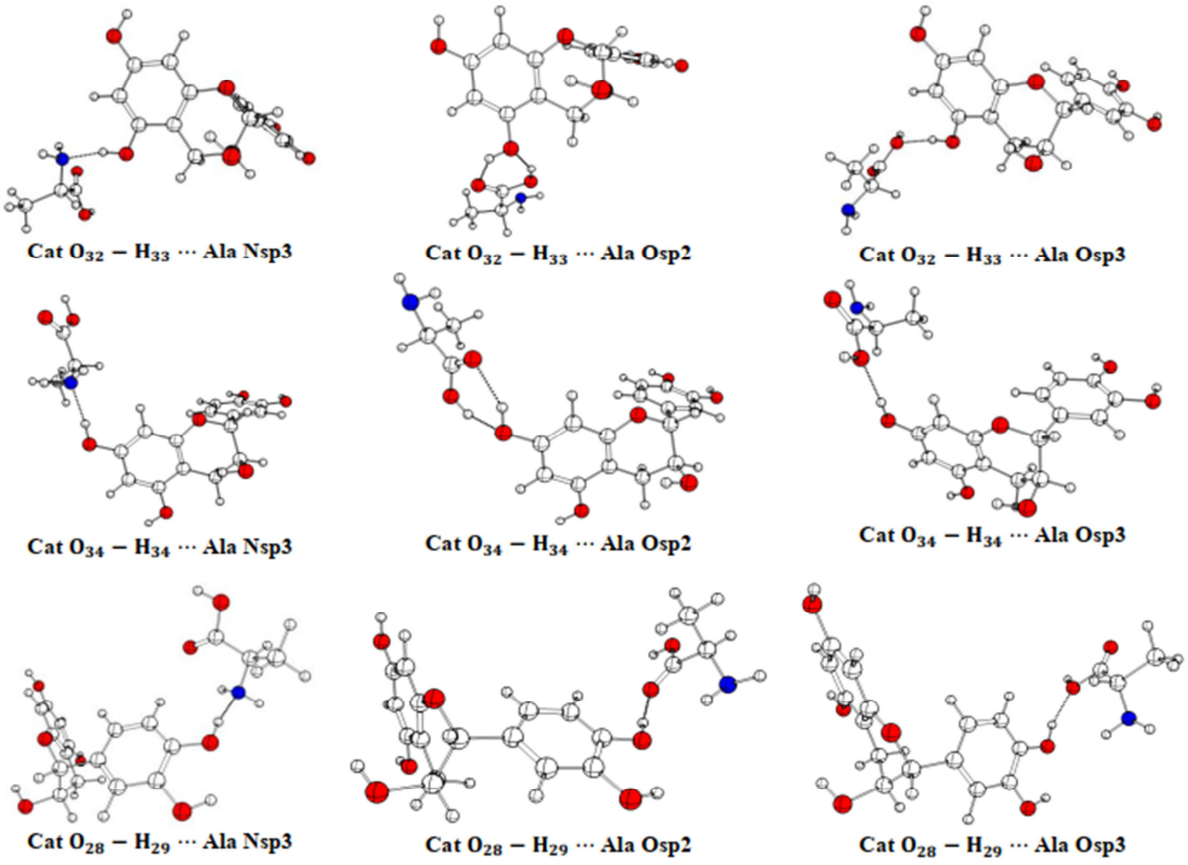

Figure 2. *Cat… Ala complexes.*

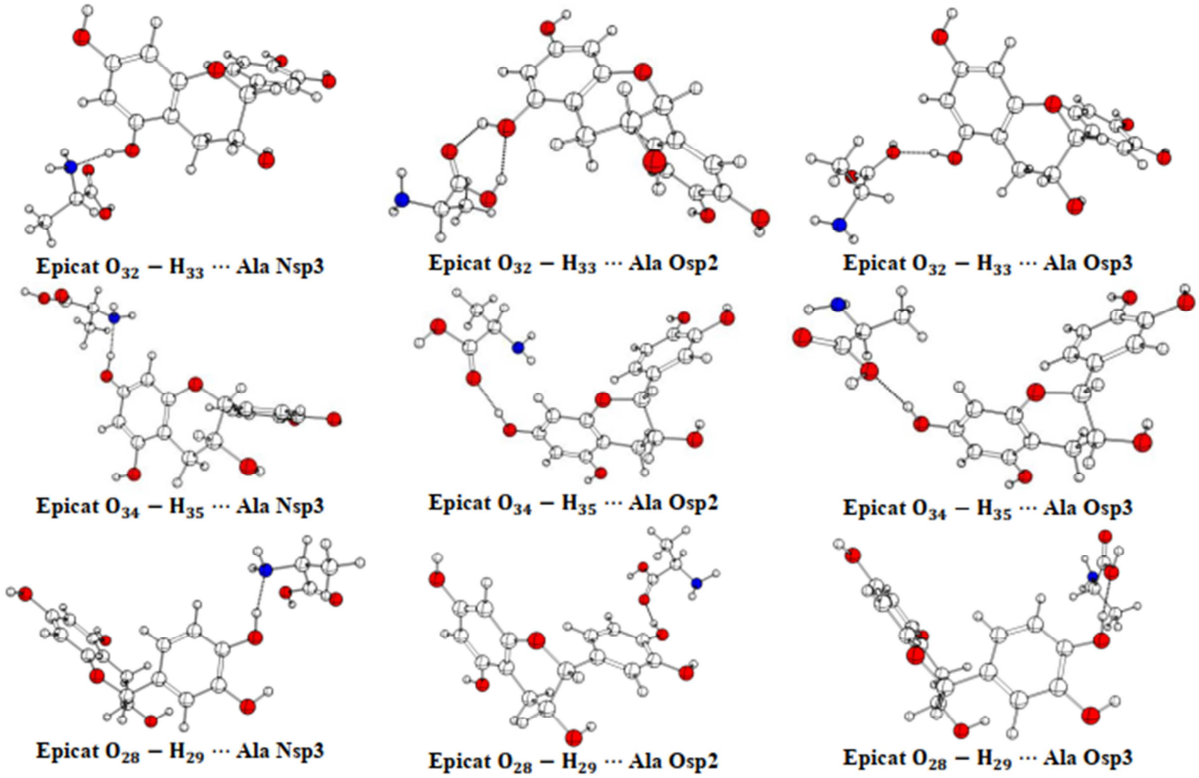

Figure 3. *EpiCat… Ala complexes.*

2.2. Interaction Energy

The interaction energy Eint is the difference between that of the entire complex and those of all its monomers; each molecular orbital is extended to a larger base than those of these. This results in excessive stabilization of this chemical structure. This energy is therefore revised using the BSSE (Basic Superposition Error) and the ZPE (zero-point energy) [35]. It is calculated from the relationship:

$$E_{int}=E_{complex}-\sum E_{monomers}+E_{BSSE}+\Delta ZPE \quad (1)$$

2.3. Nbo Analysis

The NBO method contributes to the study of intra- and intermolecular HB. It helps to clarify CT and interactions in molecular systems [36, 37]. The delocalization of electron density between the occupied bonds or lone pairs NBO orbitals and those unoccupied and antibonding corresponds to a donor-acceptor interaction. Its importance is determined using the stabilization energy$E^{(2)}$ whose expression is:

$$E^{(2)}=\Delta E_{ij}=q_i\frac{F^2(i,j)}{\varepsilon_j-\varepsilon_i} \quad (2)$$

$E^{(2)}$ measures the strength of the donor-acceptor interaction between orbitals ϕ_i and ϕ_j. The higher its value, the stronger the interaction. The second-order perturbation theory allows calculating the delocalization energy [38]. This study only takes into account $E^{(2)}$ greater than 0.15 kcal/mol.

2.4. AIM Analysis

Bader quantum theory or QTAIM is used for the topological analysis of chemical bonds [39]. In this theory, their presence between two atoms or interatomic interactions is conditioned by BCP (Bond Critical Points). The characteristics of the latter make it possible to describe the covalent or non-covalent quality of the HB. The electron density ρ (r) and its Laplacian $\nabla 2$ ρ(r), the total electron energy density H(r), the electron potential energy V(r) and the kinetic energy G(r) are commonly employed. These parameters allow categorizing the HB by their strengths. The work of Rozas et al. [40], at distinct BCP, suggests the following classification: for strong HB $\nabla^2(\rho)<0$, $H(r)<0$; for medium ones $\nabla^2(\rho)>0$, $H(r)<0$; for weak ones $\nabla^2(\rho)>0$, $H(r)>0$. The ratio - G(r)/V(r) is also used to determine the nature of the interaction at different BCP. If - G(r)/V(r) > 1, the bond is considered non-covalent [40, 41]. If 0.5 < - G(r)/V(r) < 1, it becomes partial. If - G(r)/V(r) < 0.5, it is in a closed shell. The energy of the HB is evaluated with the relation E_{HB} = - 1/2 V(r) according to the work of Espinosa [42].

2.5. NCI Analysis

The NCI analysis is a theoretical method to specify them. This specification is a function of the $(\text{sign}\,\lambda_2)\times\rho(r)$. The factor λ_2 characterizes the variation of the electron density in a perpendicular plane to the internuclear axis. $P(r)$ *represents this quantity along the latter* . It distinguishes HB from repulsive interactions (steric interactions) and Van Der Waal (VDW) ones through a 3D graphical visualization of "isosurfaces" [43–45]. NCI analysis associates non-covalent ones with the colours blue, green, and red. These correspond respectively to HB, VDW and repellent bonds. The 2D graphical visualization of the reduced density gradient as a function $(\text{sign}\,\lambda_2)\times\rho$ (r) allows us to correlate each type of interaction with the region where it appears [43–45]. Thus, the peaks linked to a negative sign of $\lambda 2\times\rho(r)$ are HB. Those at its zero value corresponding to VDW interactions. Those connected to its positive sign match with their repulsive nature.

3. Results and Discussion

3.1. Thermodynamic Parameters and Interaction Energies

Table 1 shows the energy parameters of the Cat… Ala and EpiCat… Ala. The formations of the Cat ⋯ Ala and EpiCat ⋯ Ala are in all cases spontaneous and exothermic. The complexation ΔH (enthalpies) and ΔG (free enthalpies) are all negative. The complex $CatO_i$-$H_j\cdots N_{sp^3}$, $CatO_i$-$H_j\cdots O_{sp^2}$, $EpicatO_i$-$H_j\cdots N_{sp^3}$ and $EpicatO_i$-$H_j\cdots O_{sp^2}$ exhibit relatively lower ΔH and ΔG values than the $CatO_i$-$H_j\cdots O_{sp^3}$ and $EpicatO_i$-$H_j\cdots O_{sp^3}$ complexes. Thus the N_{sp^3} and O_{sp^2} heteroatoms of Ala give more stable complexes than the O_{sp^3} heteroatom.

Interaction energies E_{int} of the complexes are all negative. For those with EpiCat ⋯ Ala (Table 1), they range from -20.60 kcal/mole to -14.56 kcal/mole for the Cat⋯ Ala and from -19.78 kcal/mole to -14.48 kcal/mole. Similar to the complexation ΔH and ΔG, interaction energies of the complex $CatO_i$-$H_j\cdots N_{sp^3}$, $CatO_i$-$H_j\cdots O_{sp^2}$, $EpicatO_i$-$H_j\cdots N_{sp^3}$ and $EpicatO_i$-$H_j\cdots O_{sp^2}$ are lower compared with those of the $CatO_i$-$H_j\cdots O_{sp^3}$ and $EpicatO_i$-$H_j\cdots O_{sp^3}$ complexes. Thus, the N_{sp^3} and O_{sp^2} sites of Ala form more stable complexes than O_{sp^3}. Among complexes formed with the N_{sp^3} site, order is $E_{int}(CatO_{34}\text{-}H_{35}\cdots N_{sp^3}) < E_{int}(CatO_{28}\text{-}H_{29}\cdots N_{sp^3}) < E_{int}(CatO_{32}\text{-}H_{33}\cdots N_{sp^3})$ for Cat and $E_{int}(EpicatO_{32}\text{-}H_{33}\cdots N_{sp^3}) < E_{int}(EpicatO_{28}\text{-}H_{29}\cdots N_{sp^3}) < E_{int}(EpicatO_{34}\text{-}H_{35}\cdots N_{sp^3})$ for EpiCat. With O_{sp^2}, ranking of interaction energies in ascending order gives: $E_{int}(CatO_{34}\text{-}H_{35}\cdots O_{sp^2}) < E_{int}(CatO_{32}\text{-}H_{33}\cdots O_{sp^2}) < E_{int}(CatO_{28}\text{-}H_{29}\cdots O_{sp^2})$ for Cat and $E_{int}(EpicatO_{32}\text{-}H_{33}\cdots O_{sp^2}) < E_{int}(EpicatO_{28}\text{-}H_{29}\cdots O_{sp^2}) < E_{int}(EpicatO_{34}\text{-}H_{35}\cdots O_{sp^2})$ for EpiCat are cited in the text.

From the above analysis, it appears that regarding Cat… Ala complexes, $CatO_{28}$-$H_{29}\cdots N_{sp^3}$, $CatO_{32}$-$H_{33}\cdots N_{sp^3}$, $CatO_{34}$-$H_{35}\cdots N_{sp^3}$, $CatO_{28}$-$H_{29}\cdots O_{sp^2}$, $CatO_{32}$-$H_{33}\cdots O_{sp^2}$ and $CatO_{34}$-$H_{35}\cdots O_{sp^2}$ are more stable. While for EpiCat … Ala complexes, $EpicatO_{28}$-$H_{29}\cdots N_{sp^3}$, $EpicatO_{32}$-$H_{33}\cdots N_{sp^3}$,

$EpicatO_{34}$-$H_{35}\cdots N_{sp^3}$, $EpicatO_{28}$-$H_{29}\cdots O_{sp^2}$, $EpicatO_{32}$-$H_{33}\cdots O_{sp^2}$ and $EpicatO_{34}$-$H_{35}\cdots O_{sp^2}$ are the most stable. NBO and AIM analyses are performed to identify the nature of the interactions that occur in these complexes.

Table 1. *Energy parameters in kcal/mol of EpiCat… Ala and Cat… Ala complexes.*

Complexes EpiCat … Ala	ΔH (kcal/mol)	ΔG	E_{int}	Complex Cat… Ala	ΔH (kcal/mol)	ΔG	E_{int}
$EpicatO_{28}$-$H_{29}\cdots N_{sp^3}$	-20.12	-10.99	-19.30	$CatO_{28}$-$H_{29}\cdots N_{sp^3}$	-21.21	-11.08	-20.32
$EpicatO_{28}$-$H_{29}\cdots O_{sp^2}$	-18.73	-9.19	-18.36	$CatO_{28}$-$H_{29}\cdots O_{sp^2}$	-18.63	-8.94	-18.27
$EpicatO_{28}$-$H_{29}\cdots O_{sp^3}$	-14.88	-6.78	-14.84	$CatO_{28}$-$H_{29}\cdots O_{sp^3}$	-14.87	-5.92	-14.56
$EpicatO_{32}$-$H_{33}\cdots N_{sp^3}$	-20.22	-11.10	-19.62	$CatO_{32}$-$H_{33}\cdots N_{sp^3}$	-20.35	-11.31	-19.76
$EpicatO_{32}$-$H_{33}\cdots O_{sp^2}$	-20.08	-10.21	-19.67	$CatO_{32}$-$H_{33}\cdots O_{sp^2}$	-19.77	-9.90	-19.34
$EpicatO_{32}$-$H_{33}\cdots O_{sp^3}$	-16.22	-7.98	-16.25	$CatO_{32}$-$H_{33}\cdots O_{sp^3}$	-14.70	-6.22	-14.64
$EpicatO_{34}$-$H_{35}\cdots N_{sp^3}$	-19.53	-10.01	-18.85	$CatO_{34}$-$H_{35}\cdots N_{sp^3}$	-21.20	-11.98	-20.60
$EpicatO_{34}$-$H_{35}\cdots O_{sp^2}$	-16.65	-7.44	-16.48	$CatO_{34}$-$H_{35}\cdots O_{sp^2}$	-20.29	-9.97	-19.84
$EpicatO_{34}$-$H_{35}\cdots O_{sp^3}$	-14.49	-6.35	-14.48	$CatO_{34}$-$H_{35}\cdots O_{sp^3}$	-14.81	-6.27	-14.85

3.2. NBO Analysis

Tables 2 to 10 provide the electronic transitions between NBO donor and acceptor sites, stabilization energies $E^{(2)}$, total stabilization energies $\sum E^{(2)}$, and CT of associated with complexes resulting from the interactions betweenO_{28}-H_{29}, O_{32}-H_{33}, O_{34}-H_{35} of Cat and EpiCat with N_{sp^3}, O_{sp^2} and O_{sp^3} of Ala NBO analysis allows us to specify, in the complexes, all interactions between Cat and Ala, on the one hand, and then between EpiCat and Ala on the other. X - H ⋯ Y is characterized by electronic transitions $LP_Y \rightarrow \sigma^*_{X\text{-}H}$ in which $\sigma^*_{X\text{-}H}$ acts as an electron acceptor and LP_Y (Y's lone pair) as an electron donor. These interactions are all defined by a second-order perturbation energy $E^{(2)}$ and a CT. In $EpicatO_{28}$-$H_{29}\cdots$Ala N_{sp^3} complex (Table 2), the total stabilization energy is $\sum E^2$ =31.09 kcal/mol. In this complex, we note the presence of the O_{28}-$H_{29}\cdots N_{39}$ HB governed by $LP^{(1)}_{N39} \rightarrow \sigma^*_{O28\text{-}H29}$ interaction. This interaction results in electron transfer from the lone pair of the nitrogen atom ($LP^{(1)}_{N39}$) to the antibonding orbital $\sigma^*_{O28\text{-}H29}$ with a stabilization energy E^2=29.9 kcal/mol and a CT of 56.64 me.O_{28}-$H_{29}\cdots N_{39}$ HB contributes 96.2% of the Epicat's total stabilization energy O_{28}-$H_{29}\cdots$Ala N_{sp^3} complex. Hence, the HB O_{28} – H_{29} ⋯ N_{39} is considered as the main interaction of the Epicat O_{28}-$H_{29}\cdots$Ala N_{sp^3} complex. Figure 4 illustrates $LP^{(1)}_{N39} \rightarrow \sigma^*_{O28\text{-}H29}$ natural bonding orbital of this main interaction. Besides the latter, the NBO analysis reveals the presence of others with low stabilization energies, including C_{36}-$H_{42}\cdots O_{28}$ (E^2=0.09 kcal/mol , CT=0.16 me), O_{28}-$H_{29}\cdots H_{45}$-N_{39} (E^2=0.62 kcal/mol , CT=0.86 me), O_{28}-$H_{29}\cdots N_{39}$-C_{37} (E^2=0.36 kcal/mol, CT=0.45 me),

The total stabilization energy of the Cat O_{28}-$H_{29}\cdots$Ala N_{sp^3} complex is $\sum E^2$ =30.53 kcal/mol(Table 2). The significant intermolecular interactions that occur are: O_{28}-$H_{29}\cdots N_{39}$, C_{22}-$H_{25}\cdots O_{40}$, C_{36}-$H_{42}\cdots O_{26}$. C_{22}-$H_{25}\cdots C_{38}$=O_{40} , O_{28}-$H_{29}\cdots H_{45}$-N_{39} and O_{28}-$H_{29}\cdots H_{46}$-N_{39} . That of O_{28}-$H_{29}\cdots N_{39}$ is 27.94 kcal/mol. This energy stabilization energy of the Cat O_{28}-$H_{29}\cdots$Ala N_{sp^3} complex accounts for 91.5% of its total value. O_{28}-$H_{29}\cdots N_{39}$ is therefore the main interaction in this complex.

Table 2. *Stabilization energies $E^{(2)}$, total stabilization energies $\sum E^{(2)}$ and CT of Epicat O_{28}-$H_{29}\cdots$Ala N_{sp^3} and Cat O_{28}-$H_{29}\cdots$Ala N_{sp^3}.*

Contact	electronic transitions	$E^{(2)}$(kcal/mol)	$\sum E^{(2)}$(kcal/mol)	CT (me)
Epicat O_{28}-$H_{29}\cdots$ Ala N_{sp^3}				
O_{28}-$H_{29}\cdots N_{39}$	$LP^{(1)}_{N39} \rightarrow \sigma^*_{O28\text{-}H29}$	29.9		56.64
C_{38}-$H_{41}\cdots O_{28}$	$LP^{(1)}_{O28} \rightarrow \sigma^*_{C38\text{-}H41}$	0.09		0.16
O_{28}-$H_{29}\cdots H_{44}$-C_{37}	$\sigma^{(1)}_{C37\text{-}H44} \rightarrow \sigma^*_{O28\text{-}H29}$	0.12	31.09	0.20
O_{28}-$H_{29}\cdots N_{39}$-C_{37}	$\sigma^{(1)}_{C37\text{-}N39} \rightarrow \sigma^*_{O28\text{-}H29}$	0.36		0.45
O_{28}-$H_{29}\cdots H_{45}$-N_{39}	$\sigma^{(1)}_{N39\text{-}H45} \rightarrow \sigma^*_{O28\text{-}H29}$	0.62		0.86
Cat O_{28}-$H_{29}\cdots$ Ala N_{sp^3}				
O_{28} – H_{29} ⋯ N_{39}	$LP^{(1)}_{N39} \rightarrow \sigma^*_{O28\text{-}H29}$	27.84		54.21
C_{22}-$H_{25}\cdots O_{40}$	$LP^{(1)}_{O40} \rightarrow \sigma^*_{C22\text{-}H25}$	0.44		0.57
	$LP^{(2)}_{O40} \rightarrow \sigma^*_{C22\text{-}H25}$	0.29	30.53	0.61
C_{22}-$H_{25}\cdots O_{40}$-C_{38}	$\pi^{(2)}_{C38\text{-}O40} \rightarrow \sigma^*_{C22\text{-}H25}$	0.35		0.60
O_{28}-$H_{29}\cdots N_{39}$-C_{37}	$\sigma^{(1)}_{C37\text{-}N39} \rightarrow \sigma^*_{O28\text{-}H29}$	0.27		0.35
O_{28}-$H_{29}\cdots H_{42}$-C_{36}	$\sigma^{(1)}_{C36\text{-}H42} \rightarrow \sigma^*_{O28\text{-}H29}$	0.1		0.17

Contact	electronic transitions	$E^{(2)}$(kcal/mol)	$\sum E^{(2)}$(kcal/mol)	CT (me)
O_{28}-H_{29}···H_{45}-N_{39}	$\sigma^{(1)}_{N39\text{-}H44} \rightarrow \sigma^{*}_{O28\text{-}H29}$	0.57		0.84
O_{28}-H_{29}···H_{46}-N_{39}	$\sigma^{(1)}_{N39\text{-}H45} \rightarrow \sigma^{*}_{O28\text{-}H29}$	0.67		0.92

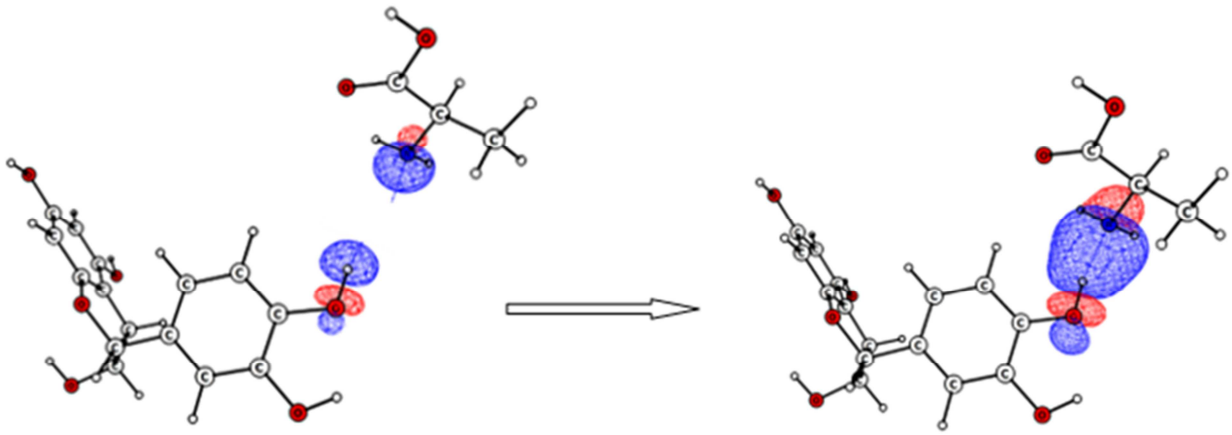

Figure 4. *Natural bond orbital of $LP^{(1)}_{N39} \rightarrow \sigma^{*}_{O28\text{-}H29}$ in O_{28}-H_{29}···N_{39} interaction.*

In the Epicat O_{28}-H_{29}···Ala O_{sp^2} complex ($\sum E^2$ =23.97 kcal/mol) (Table 3), the interactions that occur are: O_{28}-H_{29}···O_{40} , N_{39}-H_{46}···O_{28} , C_{38}-O_{40}···O_{28} , N_{39}-H_{46}···H_{29}-O_{28} , C_{22}-H_{25}···O_{40} , O_{28}-H_{29}···O_{40}-C_{38} and C_{22}-H_{25}···O_{40}-C_{38} . O_{28}-H_{29}···O_{40} is governed by two electronic relocations. These are delocalization of electrons $LP^{(1)}_{O40} \rightarrow \sigma^{*}_{O28\text{-}H29}$ (E^2=8.70 kcal/mol, CT=11.31 me) which result in their transfers from the first lone pair denoted $LP^{(1)}_{O40}$ of the oxygen to the antibonding orbital $\sigma^{*}_{O28\text{-}H29}$. It contributes 66.3% of the Epicat's total stabilization energy O_{28}-H_{29}···Ala O_{sp^2} complex. The electronic transition $LP^{(2)}_{O40} \rightarrow \sigma^{*}_{O28\text{-}H29}$ (E^2=11.51 kcal/mol, CT=23.11 me) results in the electron transfer from the second free lone pair denoted ($LP^{(2)}_{O40}$) of the oxygen atom to the antibonding orbital $\sigma^{*}_{O28\text{-}H29}$. It contributes 48% of the total stabilization energy. Thus, O_{28}-H_{29}···O_{40} contributes 84.3% of the total stabilization energy. Figure 5 provides the natural bond of the electronic transitions $LP^{(1)}_{O40} \rightarrow \sigma^{*}_{O28\text{-}H29}$ and $LP^{(2)}_{O40} \rightarrow \sigma^{*}_{O28\text{-}H29}$ of O_{28}-H_{29}···O_{40}. In Cat O_{28}-H_{29}···Ala O_{sp^2} complex whose total stabilization energy is $\sum E^2$ =23.09 kcal/mol (Table 3), the interactions that occur are: O_{28}-H_{29}···O_{40}, N_{39}-H_{46}···O_{28}, C_{22}-H_{25}···O_{40}, O_{28}-H_{29}···O_{40}-C_{38} et C_{22}-H_{25}···O_{40}-C_{38}. The O_{28}-H_{29}···O_{40} is the main interaction in this complex; its stabilization energy equals 19.83 kcal/mol, represents 84.2% of the Cat O_{28}-H_{29}···Ala O_{sp^2} complex's total value.

Table 3. *Stabilization energies $E^{(2)}$, total stabilization energies $\sum E^{(2)}$ and CT of Epicat O_{28}-H_{29}···Ala O_{sp^2} and Cat O_{28}-H_{29}···Ala O_{sp^2}.*

b	electronic transitions	$E^{(2)}$(kcal/mol)	$\sum E^{(2)}$(kcal/mol)	CT (me)
Epicat O_{28}-H_{29}··· Ala O_{sp^2}				
O_{28}-H_{29}···O_{40}	$LP^{(1)}_{O40} \rightarrow \sigma^{*}_{O28\text{-}H29}$	8.7		11.31
	$LP^{(2)}_{O40} \rightarrow \sigma^{*}_{O28\text{-}H29}$	11.51		23.11
N_{39}-H_{46}···O_{28}	$LP^{(1)}_{O28} \rightarrow \sigma^{*}_{N39\text{-}H46}$	0.64		0.92
	$LP^{(2)}_{O28} \rightarrow \sigma^{*}_{N39\text{-}H46}$	1.81		3.52
C_{38}-O_{40}···O_{28}	$LP^{(1)}_{O28} \rightarrow \pi^{*}_{C38\text{-}O40}$	0.1		0.16
N_{39}-H_{46}···H_{29}-O_{28}	$\sigma^{(1)}_{O28\text{-}H29} \rightarrow \sigma^{*}_{N39\text{-}H46}$	0.28	23.97	0.37
C_{22}-H_{25}···O_{40}	$LP^{(1)}_{O40} \rightarrow \sigma^{*}_{C22\text{-}H25}$	0.13		0.17
O_{28}-H_{29}···O_{40}-C_{38}	$\sigma^{(1)}_{C38\text{-}O40} \rightarrow \sigma^{*}_{O28\text{-}H29}$	0.38		0.38
C_{22}-H_{25}···O_{40}-C_{38}	$\pi^{(2)}_{C38\text{-}O40} \rightarrow \sigma^{*}_{C22\text{-}H25}$	0.12		0.20
O_{28}-H_{29}···O_{47}-C_{38}	$\sigma^{(1)}_{C38\text{-}O47} \rightarrow \sigma^{*}_{O28\text{-}H29}$	0.18		0.19
O_{28}-H_{29}···H_{46}-N_{39}	$\sigma^{(1)}_{N39\text{-}H46} \rightarrow \sigma^{*}_{O28\text{-}H29}$	0.12		0.16
Cat O_{28}-H_{29}··· Ala O_{sp^2}				
O_{28}-H_{29}···O_{40}	$LP^{(1)}_{O40} \rightarrow \sigma^{*}_{O28\text{-}H29}$	8.58		11.31
	$LP^{(2)}_{O40} \rightarrow \sigma^{*}_{O28\text{-}H29}$	11.25	23.54	22.58
N_{39}-H_{45}···O_{28}	$LP^{(1)}_{O28} \rightarrow \sigma^{*}_{N39\text{-}H46}$	0.67		1.01
	$LP^{(2)}_{O28} \rightarrow \sigma^{*}_{N39\text{-}H46}$	1.88		3.73

b	electronic transitions	$E^{(2)}$(kcal/mol)	$\sum E^{(2)}$(kcal/mol)	CT (me)
C_{38}-O_{40}···O_{28}	$LP^{(1)}_{O28} \rightarrow \pi^{*}_{C38\text{-}O40}$	0.1		0.16
N_{39}-H_{45}···H_{29}-O_{28}	$\sigma^{(1)}_{O28\text{-}H29} \rightarrow \sigma^{*}_{N39\text{-}H45}$	0.29		0.37
C_{22}-H_{25}···O_{40}	$LP^{(1)}_{O40} \rightarrow \sigma^{*}_{C22\text{-}H25}$	0.12		0.17
O_{28}-H_{29}···O_{40}-C_{38}	$\sigma^{(1)}_{C38\text{-}O40} \rightarrow \sigma^{*}_{O28\text{-}H29}$	0.37		0.38
O_{28}-H_{29}···O_{40}-C_{38}	$\pi^{(2)}_{C38\text{-}O40} \rightarrow \sigma^{*}_{C22\text{-}H25}$	0.11		0.20
O_{28}-H_{29}···O_{47}-C_{38}	$\sigma^{(1)}_{C38\text{-}O47} \rightarrow \sigma^{*}_{O28\text{-}H29}$	0.17		0.19

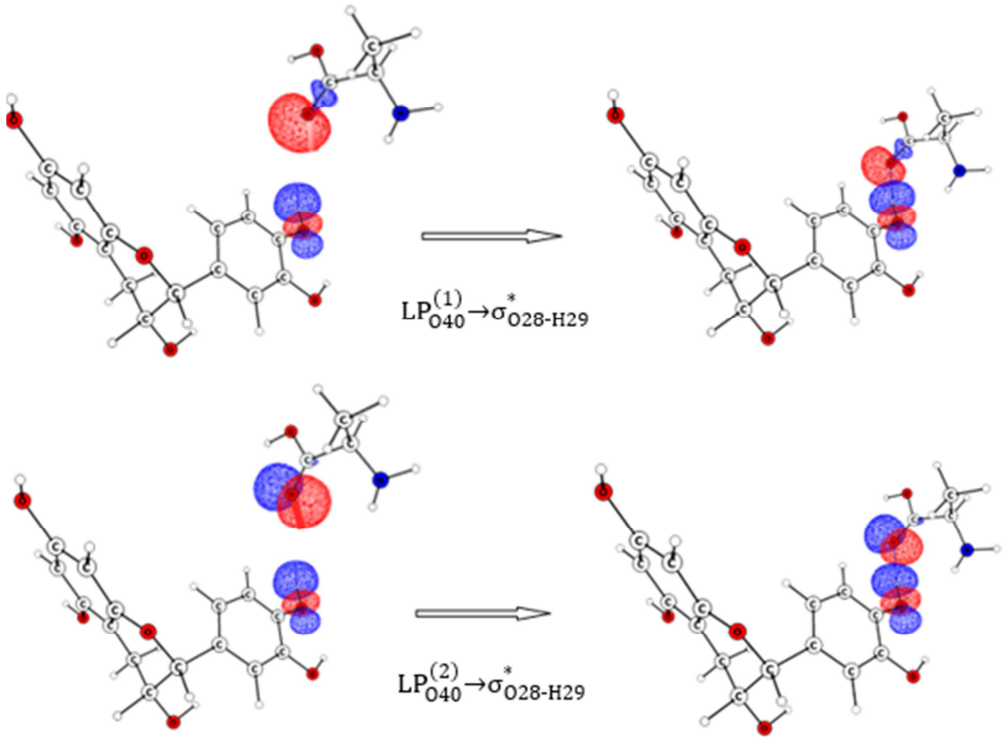

Figure 5. *Natural bond orbital of $LP^{(1)}_{O40} \rightarrow \sigma^{*}_{O28\text{-}H29}$ and $LP^{(2)}_{O40} \rightarrow \sigma^{*}_{O28\text{-}H29}$ in O_{28}-H_{29}···O_{40} interaction.*

In Epicat O_{28}-H_{29}···Ala O_{sp^3} ($\sum E^2 = 11.86$ kcal/mol) and Cat O_{28}-H_{29}···Ala O_{sp^3} ($\sum E^2 = 14.81$ kcal/mol) complexes (Table 4), the stabilization energy values of O_{28}-H_{29}···O_{47} HB are 10.95 kcal/mol and 11.66 kcal/mol, respectively. O_{28}-H_{29}···O_{47} is the main interaction in Epicat O_{28}-H_{29}···Ala O_{sp^3} and Cat O_{28}-H_{29}···Ala O_{sp^3} complexes. Other interactions involved in these complexes are:

C_{36}-H_{41}···O_{28}, C_{22}-H_{25}···O_{40}, C_{38}-O_{47}···H_{29}-O_{28}. N_{39}-H_{46}···O_{28} is the main interaction in this complex; its stabilization energy, estimated at 19.83 kcal/mol, represents 84.2% of the Cat total value.

Table 4. *Stabilization energies $E^{(2)}$, total stabilization energies $\sum E^{(2)}$ and CT of Epicat O_{28}-H_{29}···Ala O_{sp^3} and Cat O_{28}-H_{29}···Ala O_{sp^3}.*

Contact	electronic transitions	$E^{(2)}$(kcal/mol)	$\sum E^{(2)}$(kcal/mol)	CT (me)
Epicat O_{28}-H_{29}··· Ala O_{sp^3}				
O_{28}-H_{29}···O_{47}	$LP^{(1)}_{O47} \rightarrow \sigma^{*}_{O28\text{-}H29}$	10.31		14.43
	$LP^{(2)}_{O47} \rightarrow \sigma^{*}_{O28\text{-}H29}$	0.64		1.22
C_{36}-H_{41}···O_{28}	$LP^{(2)}_{O28} \rightarrow \sigma^{*}_{C36\text{-}H41}$	0.37		0.72
C_{22}-H_{25}···O_{40}	$LP^{(2)}_{O47} \rightarrow \sigma^{*}_{C22\text{-}H25}$	0.13	11.86	0.22
C_{38}-H_{47}···H_{29}-O_{28}	$\sigma^{(1)}_{O28\text{-}H29} \rightarrow \sigma^{*}_{C38\text{-}O47}$	0.15		0.21
O_{28}-H_{29}···H_{41}-C_{36}	$\sigma^{(1)}_{C36\text{-}H41} \rightarrow \sigma^{*}_{O28\text{-}H29}$	0.14		0.20
O_{28}-H_{29}···H_{48}-O_{47}	$\sigma^{(1)}_{O47\text{-}H48} \rightarrow \sigma^{*}_{O28\text{-}H29}$	0.12		0.15
Cat O_{28}-H_{29}··· Ala O_{sp^3}				
O_{28}-H_{29}···O_{47}	$LP^{(1)}_{O47} \rightarrow \sigma^{*}_{O28\text{-}H29}$	11.66		16.59
N_{39}-H_{46}···O_{28}	$LP^{(1)}_{O28} \rightarrow \sigma^{*}_{N39\text{-}H46}$	0.5	14.81	0.74
	$LP^{(2)}_{O28} \rightarrow \sigma^{*}_{N39\text{-}H46}$	2.18		4.09

Contact	electronic transitions	$E^{(2)}$(kcal/mol)	$\sum E^{(2)}$(kcal/mol)	CT (me)
C_{38}-H_{47}···H_{29}-O_{28}	$\sigma^{(1)}_{O28\text{-}H29} \rightarrow \sigma^{*}_{C38\text{-}O47}$	0.11		0.17
N_{39}-H_{46}···H_{29}-O_{28}	$\sigma^{(1)}_{O28-H29} \rightarrow \sigma^{*}_{N39-H46}$ $\sigma^{(1)}_{O28\text{-}H29} \rightarrow \sigma^{*}_{N39\text{-}H46}$	0.26		0.32
C_{22}-H_{25}···O_{47}	$LP^{(2)}_{O47} \rightarrow \sigma^{*}_{C22\text{-}H25}$	0.1		0.18

The total stabilization energy of Epicat O_{32}-H_{33}···Ala N_{sp^3} complex is ($\sum E^2$ =29.76 kcal/mol) (Table 5). In this complex, the Nsp^3 nitrogen of Ala establishes a HB with the O_{32}-H_{33} hydroxyl groups of EpiCat. This interaction O_{32}-H_{33}···N_{39} results from electron transfer from the lone pair of the nitrogen atom ($LP^{(1)}_{N36}$) to the $\sigma^{*}_{O32-H33}$ antibonding orbital which is electron depleted ($LP^{(1)}_{N39} \rightarrow \sigma^{*}_{O32\text{-}H33}$). This interaction, having energy E^2=27.32 kcal/mol, with an estimated CT of 53.92 me, contributes 91.80% of the total stabilization energy. In addition to the $O_{32} - H_{33} \cdots N_{39}$, C_1-H_7···N_{39} (E^2=0.83 kcal/mol , CT= 0.14 me), O_{32}-H_{33}···H_{45}-N_{39} (E^2=0.41 kcal/mol , CT= 0.59 me), O_{32}-H_{33}···C_{37}-N_{39} ($E^{(2)}$ = 0.45 kcal/mol , CT= 0.60 me), O_{32}-H_{33}···H_{46}-N_{39} (E^2=0.61 kcal/mol, CT= 0.84 me) the interactions contribute to the stabilization of the complex with much lower energies. The essentials for Epicat O_{32}-H_{33}···Ala N_{sp^3} is then the O_{32}-H_{33}···N_{39} . For Cat O_{32}-H_{33}···Ala N_{sp^3} , it is the O_{32}-H_{33}···N_{39} HB (Table 5). Indeed, the stabilization energy of the O_{32}-H_{33}···N_{39} is equal to 27.61kcal/mol. It represents 94.6% of the Cat total stabilization energy O_{32}-H_{33}···Ala N_{sp^3} complex ($\sum E^2$ =29.19 kcal/mol). The other interactions that occur in this complex are O_{32}-H_{33}···H_{45}-N_{39} , O_{32}-H_{33}···H_{46}-N_{39}, O_{32}-H_{33}···C_{37}-N_{39} and C_1-H_7···N_{39}. Their stabilization energies are weak.

Table 5. *Stabilization energies $E^{(2)}$, total stabilization energies $\sum E^{(2)}$ and CT of Epicat O_{32}-H_{33}···Ala N_{sp^3} and Cat O_{32}-H_{33}···Ala N_{sp^3} complexes.*

Epicat O_{32}-H_{33}··· Ala N_{sp^3}				
Contact	**electronic transitions**	**$E^{(2)}$(kcal/mol)**	**$\sum E^{(2)}$(kcal/mol)**	**CT (me)**
O_{32}-H_{33}···N_{39}	$LP^{(1)}_{N39} \rightarrow \sigma^{*}_{O32\text{-}H33}$	27.32		53.92
C_1-H_7···N_{39}	$LP^{(1)}_{N39} \rightarrow \sigma^{*}_{C1\text{-}H7}$	0.83		0.14
O_{32}-H_{33}···H_{45}-N_{39}	$\sigma^{(1)}_{N39\text{-}H45} \rightarrow \sigma^{*}_{O32\text{-}H33}$	0.41	29.76	0.59
O_{32}-H_{33}···C_{37}-N_{39}	$\sigma^{(1)}_{N39\text{-}C37} \rightarrow \sigma^{*}_{O32\text{-}H33}$	0.45		0.60
O_{32}-H_{33}···H_{46}-N_{39}	$\sigma^{(1)}_{N39\text{-}H46} \rightarrow \sigma^{*}_{O32\text{-}H33}$	0.61		0.84

Cat O_{32}-H_{33}··· Ala N_{sp^3}				
Contact	**electronic transitions**	**$E^{(2)}$(kcal/mol)**	**$\sum E^{(2)}$(kcal/mol)**	**CT (me)**
O_{32}-H_{33}···N_{39}	$LP^{(1)}_{N39} \rightarrow \sigma^{*}_{O32\text{-}H33}$	27.61		53.92
C_1-H_7···N_{39}	$LP^{(1)}_{N39} \rightarrow \sigma^{*}_{C1\text{-}H7}$	0.07		0.14
O_{32}-H_{33}···H_{45}-N_{39}	$\sigma^{(1)}_{N39\text{-}H45} \rightarrow \sigma^{*}_{O32\text{-}H33}$	0.42	29.19	0.59
O_{32}-H_{33}···C_{37}-N_{39}	$\sigma^{(1)}_{N39\text{-}C37} \rightarrow \sigma^{*}_{O32\text{-}H33}$	0.48		0.60
O_{32}-H_{33}···H_{46}-N_{39}	$\sigma^{(1)}_{N39\text{-}H46} \rightarrow \sigma^{*}_{O32\text{-}H33}$	0.61		0.84

In Epicat O_{32}-H_{33}···Ala O_{sp^2} complex ($\sum E^2$ =29.73 kcal/mol) appears two HB O_{32}-H_{33}···O_{40} and O_{47}-H_{48}···O_{32} with high stabilization energies (Table 6). O_{32}-H_{33}···O_{40} HB (E^2=13.73 kcal/mol) results in two specific electronic transitions namely $LP^{(1)}_{O40} \rightarrow \sigma^{*}_{O32\text{-}H33}$ (E^2= 4.45 kcal/mol , CT= 5.98 me) and $LP^{(2)}_{O40} \rightarrow \sigma^{*}_{O32\text{-}H33}$ (E^2=9.28 kcal/mol, CT= 20.00 me), contributing 46.2% of the total stabilization energy. Whereas, O_{47}-H_{48}···O_{32} ($E^{(2)}$ = 14.23 kcal/mol), contributes 47.9% to the total stabilization energy and is governed by electron delocalization $LP^{(1)}_{O32} \rightarrow \sigma^{*}_{O47\text{-}H48}$ (E^2=6.10 kcal/mol , CT= 9.61 me) and $LP^{(2)}_{O32} \rightarrow \sigma^{*}_{O47\text{-}H48}$ (E^2=8.13 kcal/mol, CT= 17.00 me). These two HB O_{32}-H_{33}···O_{40} and O_{47}-H_{48}···O_{32} constitute the main interactions of Epicat O_{32}-H_{33}···Ala O_{sp^2} complex. However, it is important to note the presence of other interactions including O_{47}-H_{48}···C_2-C_1 , O_{47}-H_{48}···H_{33}-O_{32} , O_{32}-H_{33}···O_{40}-C_{38} . The total stabilization energy of the Cat O_{32}-H_{33}···Ala O_{sp^2} complex is $\sum E^2$ =30.63 kcal/mol (Table 6). The intermolecular interactions that most stabilize this complex are: O_{32}-H_{33}···O_{40} and O_{47}-H_{48}···O_{32} . Their stabilization energies are 14.43 kcal/mol and 14.24 kcal/mol, respectively.

The total stabilization energies of Epicat O_{32}-H_{33}···Ala O_{sp^3} and Cat O_{32}-H_{33}···Ala O_{sp^3} complexes are 10.71 kcal/mol and 10.93 kcal/mol respectively (Table 7). The interactions that occur in these complexes are O_{32}-H_{33}···O_{47}, C_{37}-H_{44}···O_{32}, O_{36}-H_{43}···C_2-C_1, C_1-H_7···O_{47} and O_{32}-H_{33}···H_{48}-O_{47} . In Epicat O_{32}-H_{33}···Ala O_{sp^3} complex, the stabilization energy

of O_{32}-$H_{33}\cdots O_{47}$ is 10.2 kcal/mol and represents 95.3% of $\sum E^{(2)}$. This energy is equal to 10.52 kcal/mol and represents 96.2% of $\sum E^{(2)}$ in Cat O_{32}-$H_{33}\cdots$Ala O_{sp^3} complex. Thus, the main interaction of Epicat O_{32}-$H_{33}\cdots$Ala O_{sp^3} and Cat O_{32}-$H_{33}\cdots$Ala O_{sp^3} complexes is O_{32}-$H_{33}\cdots O_{47}$.

In Epicat O_{34}-$H_{35}\cdots$Ala N_{sp^3} complex ($\sum E^2$ =27.31 kcal/mol) (Table 8), we note the presence of the O_{34}-$H_{35}\cdots N_{39}$, C_{36}-$H_{42}\cdots O_{34}$, C_5-$H_8\cdots N_{39}$ HB and other interactions with low stabilization energies. O_{34}-$H_{35}\cdots N_{39}$ HB is resulted in the electronic transition $LP^{(1)}_{N39}\rightarrow\sigma^*_{O34\text{-}H35}$ ($E^{(2)}$= 25.64 kcal/mol, CT= 50.73 me). It accounts for 93.9% of the total stabilization energy. O_{34}-$H_{35}\cdots N_{39}$ is considered the main interaction of the Epicat O_{34}-$H_{35}\cdots$Ala N_{sp^3} complex. The total stabilization energy of the Cat O_{34}-$H_{35}\cdots$Ala N_{sp^3} complex is $\sum E^2$ =28.93 kcal/mol. The intermolecular interactions that stabilize this complex most strongly is O_{34}-$H_{35}\cdots N_{39}$. His stabilization energy is worth 27.14 kcal/mol.

Table 6. *Stabilization energies $E^{(2)}$, total stabilization energies $\sum E^{(2)}$ and CT of Epicat O_{32}-$H_{33}\cdots$Ala O_{sp^2} and Cat O_{32}-$H_{33}\cdots$Ala O_{sp^2}.*

Epicat O_{32}-$H_{33}\cdots$ Ala O_{sp^2}				
Contact	**electronic transitions**	**$E^{(2)}$(kcal/mol)**	**$\sum E^{(2)}$(kcal/mol)**	**CT (me)**
O_{47}-$H_{48}\cdots O_{32}$	$LP^{(1)}_{O32}\rightarrow\sigma^*_{O47\text{-}H48}$	6.1		9.61
	$LP^{(2)}_{O32}\rightarrow\sigma^*_{O47\text{-}H48}$	8.13		17.00
O_{32}-$H_{33}\cdots O_{40}$	$LP^{(1)}_{O40}\rightarrow\sigma^*_{O32\text{-}H33}$	4.45		5.98
	$LP^{(2)}_{O40}\rightarrow\sigma^*_{O32\text{-}H33}$	9.28		20.00
O_{47}-$H_{48}\cdots C_2$-C_1	$\sigma^{(1)}_{C1\text{-}C2}\rightarrow\sigma^*_{O47\text{-}H48}$	0.11	29.73	0.15
O_{47}-$H_{48}\cdots H_{33}$-O_{32}	$\sigma^{(1)}_{O32\text{-}H33}\rightarrow\sigma^*_{O47\text{-}H48}$	1.06		1.42
O_{32}-$H_{33}\cdots C_{38}$-C_{37}	$\sigma^{(1)}_{C37\text{-}C38}\rightarrow\sigma^*_{O32\text{-}H33}$	0.19		0.28
O_{32}-$H_{33}\cdots O_{40}$-C_{38}	$\sigma^{(1)}_{C38\text{-}O40}\rightarrow\sigma^*_{O32\text{-}H33}$	0.23		0.25
C_2-$O_{32}\cdots H_{48}$-O_{47}	$\sigma^{(1)}_{O47\text{-}H48}\rightarrow\sigma^*_{C2\text{-}O32}$	0.18		0.27

Cat O_{32}-$H_{33}\cdots$ Ala O_{sp^2}				
Contact	**electronic transitions**	**$E^{(2)}$(kcal/mol)**	**$\sum E^{(2)}$(kcal/mol)**	**CT (me)**
O_{47}-$H_{48}\cdots O_{32}$	$LP^{(1)}_{O32}\rightarrow\sigma^*_{O47\text{-}H48}$	6.63		10.24
	$LP^{(2)}_{O32}\rightarrow\sigma^*_{O47\text{-}H48}$	7.61		15.60
O_{32}-$H_{33}\cdots O_{40}$	$LP^{(1)}_{O40}\rightarrow\sigma^*_{O32\text{-}H33}$	4.56		6.28
	$LP^{(2)}_{O40}\rightarrow\sigma^*_{O32\text{-}H33}$	9.87		21.10
O_{47}-$H_{48}\cdots C_2$-C_1	$\sigma^{(1)}_{C1\text{-}C2}\rightarrow\sigma^*_{O47\text{-}H48}$	0.11	30.63	0.15
O_{47}-$H_{48}\cdots H_{33}$-O_{32}	$\sigma^{(1)}_{O32\text{-}H33}\rightarrow\sigma^*_{O47\text{-}H48}$	1.1		1.42
C_2-$O_{32}\cdots O_{40}$	$LP^{(2)}_{O40}\rightarrow\sigma^*_{C2\text{-}O32}$	0.11		0.24
O_{32}-$H_{33}\cdots C_{38}$-O_{40}	$\sigma^{(1)}_{C38\text{-}O40}\rightarrow\sigma^*_{O32\text{-}H33}$	0.25		0.25
O_{32}-$H_{33}\cdots C_{37}$-C_{38}	$\sigma^{(1)}_{C38\text{-}C37}\rightarrow\sigma^*_{O32\text{-}H33}$	0.19		0.28
C_2-$O_{32}\cdots H_{48}$-O_{47}	$\sigma^{(1)}_{O47\text{-}H48}\rightarrow\sigma^*_{C2\text{-}O32}$	0.2		0.27

Table 7. *Stabilization energies $E^{(2)}$, total stabilization energies $\sum E^{(2)}$ and CT of Epicat O_{32}-$H_{33}\cdots$Ala O_{sp^3} and Cat O_{32}-$H_{33}\cdots$Ala O_{sp^3} complexes.*

Epicat O_{32}-$H_{33}\cdots$ Ala O_{sp^3}				
Contact	**electronic transitions**	**$E^{(2)}$(kcal/mol)**	**$\sum E^{(2)}$(kcal/mol)**	**CT (me)**
O_{32}-$H_{33}\cdots O_{47}$	$LP^{(1)}_{O47}\rightarrow\sigma^*_{O32\text{-}H33}$	9		12.69
	$LP^{(2)}_{O47}\rightarrow\sigma^*_{O32\text{-}H33}$	1.2		2.17
C_{37}-$H_{44}\cdots O_{32}$	$LP^{(2)}_{O32}\rightarrow\sigma^*_{C37\text{-}H44}$	0.22	10.71	0.44
C_{36}-$H_{43}\cdots C_2$-C_1	$\pi^{(2)}_{C1\text{-}C2}\rightarrow\sigma^*_{C36\text{-}H43}$	0.07		0.15
C_1-$H_7\cdots O_{47}$	$LP^{(1)}_{O47}\rightarrow\sigma^*_{C1\text{-}H7}$	0.13		0.19
	$LP^{(2)}_{O47}\rightarrow\sigma^*_{C1\text{-}H7}$	0.09		0.18

Cat O_{32}-$H_{33}\cdots$ Ala O_{sp^3}				
Contact	**electronic transitions**	**$E^{(2)}$(kcal/mol)**	**$\sum E^{(2)}$(kcal/mol)**	**CT (me)**
O_{32}-$H_{33}\cdots O_{47}$	$LP^{(1)}_{O47}\rightarrow\sigma^*_{O32\text{-}H33}$	7.64		10.79
	$LP^{(2)}_{O47}\rightarrow\sigma^*_{O32\text{-}H33}$	2.88	10.93	5.36
C_1-$H_7\cdots O_{47}$	$LP^{(1)}_{O47}\rightarrow\sigma^*_{C1\text{-}H7}$	0.13		0.19

Cat O_{32}-H_{33}··· Ala O_{sp^3}				
Contact	**electronic transitions**	**$E^{(2)}$(kcal/mol)**	**$\sum E^{(2)}$(kcal/mol)**	**CT (me)**
C_{36}-H_{43}···C_2-C_1	$\pi^{(2)}_{C1\text{-}C2} \rightarrow \sigma^{*}_{C36\text{-}H43}$	0.17		0.40
O_{32}-H_{33}···H_{48}-O_{47}	$\sigma^{(1)}_{O47\text{-}H48} \rightarrow \sigma^{*}_{O32\text{-}H38}$	0.11		0.13

In the case of Epicat O_{34}-H_{35}···Ala O_{sp^2} complex ($\sum E^2$ =23.84 kcal/mol) (Table 9), appear the interactions O_{34}-H_{35}···O_{40}, O_{47}-H_{48}···C_5-C_6 as well as other interactions with low stabilization energies such as O_{47}-H_{48}···H_8-C_5, O_{34}-H_{35}···O_{40}-C_{38}. O_{34}-H_{35}···O_{40} is characterized by the electronic transitions $LP^{(1)}_{40} \rightarrow \sigma^{*}_{O34\text{-}H35}$ ($E^{(2)}$= 7.73 kcal/mol, CT= 10.27 me) et $LP^{(2)}_{40} \rightarrow \sigma^{*}_{O34\text{-}H35}$ ($E^{(2)}$= 7.74 kcal/mol, CT= 16.06 me). It contributes 62.10% to the total stabilization energy of the complex. Similarly, O_{47}-H_{48}···C_5-C_6 interaction is governed by two electronic transitions that are $\sigma^{(1)}_{C5\text{-}C6} \rightarrow \sigma^{*}_{O44\text{-}H45}$ ($E^{(2)}$= 0.19 kcal/mol, CT= 0.26 me) et $\pi^{(2)}_{C5\text{-}C6} \rightarrow \sigma^{*}_{O44\text{-}H45}$ ($E^{(2)}$= 6.13 kcal/mol, CT= 14.55 me). In Cat O_{34}-H_{35}···Ala O_{sp^2} complex, the total stabilization energy is 30.14 kcal/mol. The HB O_{34}-H_{35}···O_{40} ($E^{(2)}$= 14.06 kcal/mol, CT= 26.28 me) et O_{47}-H_{48}···O_{34} ($E^{(2)}$= 14.18 kcal/mol, CT= 26.41 me) together account for 98.7% of the Cat total stabilization energy O_{34}-H_{35}···Ala O_{sp^2} complex and are its main interactions.

Table 8. *Stabilization energies $E^{(2)}$, total stabilization energies $\sum E^{(2)}$ and CT of Epicat O_{34}-H_{35}··· Ala N_{sp^3} and Cat O_{34}-H_{35}··· Ala N_{sp^3} complexes.*

Epicat O_{34}-H_{35}··· Ala N_{sp^3}				
Contact	**electronic transitions**	**$E^{(2)}$(kcal/mol)**	**$\sum E^{(2)}$(kcal/mol)**	**CT (me)**
O_{34}-H_{35}···N_{39}	$LP^{(1)}_{N39} \rightarrow \sigma^{*}_{O34\text{-}H35}$	25.64		50.73
C_{36}-H_{42}···O_{34}	$LP^{(1)}_{O34} \rightarrow \sigma^{*}_{C36\text{-}H42}$	0.22		0.34
C_5-H_8···N_{39}	$LP^{(1)}_{N39} \rightarrow \sigma^{*}_{C5\text{-}H8}$	0.06		0.10
O_{34}-H_{35}···H_{44}-C_{37}	$\sigma^{(1)}_{C37\text{-}H44} \rightarrow \sigma^{*}_{O34\text{-}H35}$	0.1	27.31	0.16
O_{34}-H_{35}···N_{39}-C_{37}	$\sigma^{(1)}_{C37\text{-}N39} \rightarrow \sigma^{*}_{O34\text{-}H35}$	0.26		0.36
O_{34}-H_{35}···H_{45}-N_{39}	$\sigma^{(1)}_{N39\text{-}H45} \rightarrow \sigma^{*}_{O34\text{-}H35}$	0.5		0.72
O_{34}-H_{35}···H_{46}-N_{39}	$\sigma^{(1)}_{N39\text{-}H46} \rightarrow \sigma^{*}_{O34\text{-}H35}$	0.53		0.79

Cat O_{34}-H_{35}··· Ala N_{sp^3}				
Contact	**electronic transitions**	**$E^{(2)}$(kcal/mol)**	**$\sum E^{(2)}$(kcal/mol)**	**CT (me)**
O_{34}-H_{35}···N_{39}	$LP^{(1)}_{N39} \rightarrow \sigma^{*}_{O34\text{-}H35}$	27.14		53.92
C_{36}-H_{43}···O_{34}	$LP^{(1)}_{O34} \rightarrow \sigma^{*}_{C36\text{-}H42}$	0.27		0.60
C_5-H_8···N_{39}	$LP^{(1)}_{N39} \rightarrow \sigma^{*}_{C5\text{-}H8}$	0.08	28.93	0.14
O_{34}-H_{35}···N_{39}-C_{37}	$\sigma^{(1)}_{C37\text{-}N39} \rightarrow \sigma^{*}_{O34\text{-}H35}$	0.39		0.49
O_{34}-H_{35}···H_{45}-N_{39}	$\sigma^{(1)}_{N39\text{-}H45} \rightarrow \sigma^{*}_{O34\text{-}H35}$	0.58		0.86
O_{34}-H_{35}···H_{46}-N_{39}	$\sigma^{(1)}_{N39\text{-}H46} \rightarrow \sigma^{*}_{O34\text{-}H35}$	0.47		0.65

Table 9. *Stabilization energies $E^{(2)}$, total stabilization energies $\sum E^{(2)}$ and CT of Epicat O_{34}-H_{35}··· Ala O_{sp^2} and Cat O_{34}-H_{35}··· Ala O_{sp^2}.*

Epicat O_{34}-H_{35}··· Ala O_{sp^2}				
Contact	**electronic transitions**	**$E^{(2)}$**	**$\sum E^{(2)}$**	**CT**
O_{34}-H_{35}···O_{40}	$LP^{(1)}_{O40} \rightarrow \sigma^{*}_{O34\text{-}H35}$	7.73		10.27
	$LP^{(2)}_{O40} \rightarrow \sigma^{*}_{O34\text{-}H35}$	7.74		16.06
C_5-H_8···O_{40}	$LP^{(2)}_{O40} \rightarrow \sigma^{*}_{C5\text{-}H8}$	0.1		0.22
O_{47}-H_{48}···C_5-C_4	$\sigma^{(1)}_{C4\text{-}C5} \rightarrow \sigma^{*}_{O47\text{-}H48}$	0.12		0.16
O_{47}-H_{48}···C_6-C_5	$\sigma^{(1)}_{C5\text{-}C6} \rightarrow \sigma^{*}_{O47\text{-}H48}$	0.19	23.84	0.26
	$\pi^{(2)}_{C5-C6} \rightarrow \sigma^{*}_{O47\text{-}H48}$	6.13		14.55
O_{47}-H_{48}···H_8-C_5	$\sigma^{(1)}_{C5\text{-}H8} \rightarrow \sigma^{*}_{O47\text{-}H48}$	1.2		1.99
C_{38}-O_{40}···H_{35}-O_{34}	$\sigma^{(1)}_{O34\text{-}H35} \rightarrow \pi^{(2)*}_{C38\text{-}O40}$	0.14		0.31
O_{34}-H_{35}···C_{38}-C_{37}	$\sigma^{(1)}_{C37\text{-}C38} \rightarrow \sigma^{*}_{O34\text{-}H35}$	0.2		0.26
O_{34}-H_{35}···O_{40}-C_{38}	$\sigma^{(1)}_{C38\text{-}O40} \rightarrow \sigma^{*}_{O34\text{-}H35}$	0.29		0.29

Cat O_{34}-H_{35}··· Ala O_{sp^2}				
Contact	**electronic transitions**	$E^{(2)}$	$\sum E^{(2)}$	**CT**
O_{34}-H_{35}···O_{40}	$LP^{(1)}_{O40} \rightarrow \sigma^{*}_{O34\text{-}H35}$	4.58		6.28
	$LP^{(2)}_{O40} \rightarrow \sigma^{*}_{O34\text{-}H35}$	9.48		20.00
O_{47}-H_{48}···O_{34}	$LP^{(1)}_{O34} \rightarrow \sigma^{*}_{O47\text{-}H48}$	6.22		9.88
	$LP^{(2)}_{O34} \rightarrow \sigma^{*}_{O47\text{-}48}$	7.96		16.53
O_{47}-H_{48}···C_6-C_5	$\sigma^{(1)}_{C5\text{-}C6} \rightarrow \sigma^{*}_{O47\text{-}H48}$	0.09	30.14	0.12
O_{47}-H_{48}···H_{35}-O_{34}	$\sigma^{(1)}_{O34\text{-}H35} \rightarrow \sigma^{*}_{O47\text{-}H48}$	1.05		1.45
C_6-O_{34}···O_{40}	$LP^{(2)}_{O40} \rightarrow \sigma^{*}_{C6\text{-}O34}$	0.11		0.24
O_{34}-H_{35}···C_{38}-C_{37}	$\sigma^{(1)}_{C37\text{-}C38} \rightarrow \sigma^{*}_{O34\text{-}H35}$	0.2		0.28
O_{34}-H_{35}···O_{40}-C_{38}	$\sigma^{(1)}_{C38\text{-}O40} \rightarrow \sigma^{*}_{O34\text{-}H35}$	0.25		0.25
C_6-O_{34}···H_{48}-O_{47}	$\sigma^{(1)}_{O47\text{-}H48} \rightarrow \sigma^{*}_{C6\text{-}O34}$	0.2		0.27

The stabilization energy of the O_{34}-H_{35}···O_{47} HB is 9.96 kcal/mol in the Epicat O_{34}-H_{35}···Ala O_{sp^3} complex ($\sum E^2 = 10.40$ kcal/mol) and 9.50 kcal/mol in the Cat O_{34}-H_{35}···Ala O_{sp^2} complex ($\sum E^2 = 10.03$ kcal/mol) (Table 10). These values account for approximately 95% of these two complexes total stabilization energy. The O_{34}-H_{35}···O_{47} is thus their main interaction. The others are weak. They comprise C_5-H_8···O_{47} , C_{36}-H_{41}···O_{34} , O_{34}-H_{35}···H_{44}-C_{37}…

The NBO analysis makes it possible to specify all the interactions between Epicat or Cat and Ala in all the complexes. In the latter, in addition to the bonds X - H ··· Y (X = O, N, C; Y = O, N), several other interactions appear. These include O - H ··· C = O, O - H ··· C = C, C - H ··· C = C, O - H ··· H - O, C - H ··· H - C, N - H ··· H - O, O - H ··· H - C. X - H ··· Y is characterized by CT $LP_Y \rightarrow \sigma^{*}_{X-H}$ in which σ^{*}_{X-H} acts as electron acceptor and LP_Y as an electron donor. The O - H ··· O, O - H ··· N and N - H ··· O HB are the main ones for EpiCat… Ala and Cat… Ala complexes. For this latter, interactions with the N_{sp^3} and O_{sp^2} heteroatoms are stronger than those with O_{sp^3}. They have the most intense stabilization energies $E^{(2)}$.

Table 10. *Stabilization energies $E^{(2)}$, total stabilization energies $\sum E^{(2)}$ and CT of Epicat O_{34}-H_{35}···Ala O_{sp^3} and Cat O_{34}-H_{35}···Ala O_{sp^3}.*

Epicat O_{34}-H_{35}··· Ala O_{sp^3}				
Contact	**electronic transitions**	$E^{(2)}$**(kcal/mol)**	$\sum E^{(2)}$**(kcal/mol)**	**CT (me)**
O_{34}-H_{35}···O_{47}	$LP^{(1)}_{O47} \rightarrow \sigma^{*}_{O34\text{-}H35}$	7.51		10.53
	$LP^{(2)}_{O47} \rightarrow \sigma^{*}_{O34\text{-}H35}$	2.44		4.65
C_{36}-H_{41}···O_{34}	$LP^{(2)}_{O34} \rightarrow \sigma^{*}_{C36\text{-}H41}$	0.06		0.12
C_{36}-H_{41}···C_6-C_5	$\pi^{(2)}_{C5-C6} \rightarrow \sigma^{*}_{C36\text{-}H41}$	0.08	10.40	0.19
C_5-H_8···O_{47}	$LP^{(1)}_{O47} \rightarrow \sigma^{*}_{C5\text{-}H8}$	0.15		0.19
	$LP^{(2)}_{O47} \rightarrow \sigma^{*}_{C5\text{-}H8}$	0.05		0.10
O_{34}-H_{35}···H_{48}-O_{47}	$\sigma^{(1)}_{O47\text{-}H48} \rightarrow \sigma^{*}_{O34\text{-}H35}$	0.11		0.15

Cat O_{34}-H_{35}··· Ala O_{sp^3}				
Contact	**electronic transitions**	$E^{(2)}$**(kcal/mol)**	$\sum E^{(2)}$**(kcal/mol)**	**CT (me)**
O_{34}-H_{35}···O_{47}	$LP^{(1)}_{O47} \rightarrow \sigma^{*}_{O34\text{-}H35}$	9.14		12.97
	$LP^{(2)}_{O47} \rightarrow \sigma^{*}_{O34\text{-}H35}$	0.36		0.71
C_{37}-H_{44}···O_{34}	$LP^{(2)}_{O34} \rightarrow \sigma^{*}_{C37\text{-}H44}$	0.18	10.03	0.37
C_5-H_8···O_{47}	$LP^{(1)}_{O47} \rightarrow \sigma^{*}_{C5\text{-}H8}$	0.12		0.16
	$LP^{(2)}_{O47} \rightarrow \sigma^{*}_{C5\text{-}H8}$	0.14		0.28
O_{34}-H_{35}···H_{44}-C_{37}	$\sigma^{(1)}_{C37\text{-}H44} \rightarrow \sigma^{*}_{O34\text{-}H35}$	0.09		0.16

3.3. Geometric and Spectroscopic Parameters

Tables 11 and 12 summarize some geometric and spectroscopic parameters of X - H ··· Y in EpiCat … Ala and Cat … Ala complexes, respectively. They show the bond distances and angles between interacting atoms, the stretching frequencies of O-H, N-H and C-H and their variations. The results indicate that for O - H ··· O, O - H ··· N and N - H ··· O HB, the fluctuations in the lengths of the hydroxyl groups (Δd_{O-H}) and those of the N - H group (Δd_{N-H}) are positive (Tables 11 and 12). These O - H and N - H bond elongations result from the CT of the LP_Y the electron-rich proton acceptor Y (Y = O, N) to the antibonding orbital $\sigma^{*}_{X\text{-}H}$ of X - H (X = O, N, C). This is the $LP_Y \rightarrow \sigma^{*}_{X\text{-}H}$ electronic transition. This result is consistent with the conclusions of Albugin and al. [46]. These CT are explained by the reduction of the elongation

(redshift) frequencies of O-H and N-H ($\Delta\nu_{O\text{-}H} < 0$ and $\Delta\nu_{N\text{-}H} < 0$). From this fact, all O - H ⋯ O, O - H ⋯ N and N - H ⋯ O interactions are proper HB [47.48]. O - H ⋯ O and O - H ⋯ N exhibit intermolecular distance d (H⋯O) and d (H⋯N) between 1.79761 Å and 1.97709 Å and then linearity angles ∠ XHY ranging from 139.4° to 176.6°. These data are in keeping with those of moderate HB (1.5 Å <d (H⋯O) <2.2 Å and 130° < ∠XHY < 180°) [49.50]. In contrast, for N - H ⋯ O, d (H⋯O) is between 2.35220 Å and 3.36209 Å with ∠XHY between 147.3° and 154.9°. These values suggest that the N - H ⋯ O is weak in these complexes. The last column of Table 11 or 12 shows the strengths of HB in these due to both the contraction of the C - H bonds and the increase in its elongation frequency (blue shift) ($\Delta d_{C-H} < 0$ and $\Delta\nu_{C\text{-}H} > 0$). C - H ⋯ Y interactions are improper or unconventional HB [47.48]. For these, the intermolecular distance d (H⋯O) and d (H⋯N) and the linearity angles ∠ XHY are between 2.64825 and 3.58144 Å and then between 119.2° and 158.8° respectively. These values indicate that these improper HB are weak.

Table 11. *Geometric parameters of the X - H ⋯ Y interactions (distance in Å, angle in degree) and the elongation frequencies υ (cm^{-1}) of the X - H bonds in Cat ⋯Ala complexes and their variation Δυ (cm^{-1}).*

Complexes	Contact	d(H⋯Y) (Å)	∠XHY(°)	Δd(X-H) (Å)	$\Delta\nu_{X\text{-}H}$ (cm^{-1})
Cat O_{28}-H_{29}⋯Ala N_{sp^3}	O_{28}-H_{29}⋯N_{39}	1.81368	169.5	0.02911	-598.3
	C_{22}-H_{25}⋯O_{40}	2.64825	158.8	-0.00183	24.1
	C_{36}-H_{42}⋯O_{28}	2.98252	119.2	-0.00171	19.9
Cat O_{28}-H_{29}⋯Ala O_{sp^2}	O_{28}-H_{29}⋯O_{40}	1.80941	167.9	0.01485	-291.3
	N_{39}-H_{45}⋯O_{28}	2.35220	147.7	0.00107	-9.1
	O_{22}-H_{25}⋯O_{40}	2.87216	123.1	-0.00158	20.6
Cat O_{28}-H_{29}⋯Ala O_{sp^3}	O_{28}-H_{29}⋯O_{47}	1.91027	162.8	0.00827	-160.2
	N_{39}-H_{46}⋯O_{28}	2.36209	154.8	0.00174	0.3
	C_{22}-H_{25}⋯O_{47}	3.58144	130.0	-0.00101	12.5
Cat O_{32}-H_{33}⋯Ala N_{sp^3}	O_{32}-H_{33}⋯N_{39}	1.81460	166.0	0.02773	-570.3
	C_1-H_7⋯N_{39}	3.05293	120.9	-0.00168	19.1
Cat O_{32}-H_{33}⋯Ala O_{sp^2}	O_{32}-H_{33}⋯O_{40}	1.89987	139.5	0.01517	-268.7
	O_{47}-H_{48}⋯O_{32}	1.85602	153.2	0.01305	-276.1
Cat O_{32}-H_{33}⋯Ala O_{sp^3}	O_{32}-H_{33}⋯O_{47}	1.96426	169.3	0.00591	-118.9
	C_1-H_7⋯O_{47}	3.01039	124.9	-0.00091	12.6
Cat O_{34}-H_{35}⋯Ala N_{sp^3}	O_{34}-H_{35}⋯N_{39}	1.82916	170.9	0.02664	-547.2
	C_{36}-H_{43}⋯O_{34}	2.92218	126.6	-0.00237	12.0
	C_5-H_8⋯N_{39}	2.97692	121.9	-0.00189	20.6
Cat O_{34}-H_{35}⋯Ala O_{sp^2}	O_{34}-H_{35}⋯O_{40}	1.90542	139.8	0.01469	-259.6
	O_{47}-H_{48}⋯O_{34}	1.86270	153.3	0.01354	-280.4
Cat O_{34}-H_{35}⋯Ala O_{sp^3}	O_{34}-H_{35}⋯O_{47}	1.97331	171.9	0.00552	-106.2
	C_5-H_8⋯O_{47}	2.95605	125.4	-0.00105	13.3

Table 12. *Geometric parameters of the X - H ⋯ Y interactions (distance in Å, angle in degree) and the elongation frequencies υ (cm^{-1}) of the X - H bonds in EpiCat ⋯Ala complexes and their variation Δυ (cm^{-1}).*

Complexes	Contact	d(H⋯Y) (Å)	∠XHY(°)	Δd(X-H) (Å)	$\Delta\nu_{X\text{-}H}$ (cm^{-1})
Epicat O_{28}-H_{29}⋯Ala N_{sp^3}	O_{28}-H_{29}⋯N_{39}	1.79761	171.1	0.03092	-634.8
	O_{36}-H_{41}⋯O_{28}	2.96005	123.7	-0.002	92.8
Epicat O_{28}-H_{29}⋯Ala O_{sp^2}	O_{28}-H_{29}⋯O_{40}	1.80454	168.2	0.01523	-299.1
	N_{39}-H_{45}⋯O_{28}	2.36187	147.3	0.00096	-8.8
	C_{22}-H_{25}⋯O_{43}	2.85709	123.2	-0.00157	20.5
Epicat O_{28}-H_{29}⋯Ala O_{sp^3}	O_{28}-H_{29}⋯O_{47}	1.93377	172.6	0.00702	-138.7
	O_{36}-H_{41}⋯O_{28}	2.85381	150.7	-0.00274	19.6
	C_{22}-H_{25}⋯O_{47}	3.04357	124.2	-0.00103	12.6
Epicat O_{32}-H_{33}⋯Ala N_{sp^3}	O_{32}-H_{33}⋯N_{39}	1.81873	167.0	0.02739	-562.9
	C_1-H_7⋯N_{39}	2.93336	128.2	-0.00167	18.4
Epicat O_{32}-H_{33}⋯Ala O_{sp^2}	O_{47}-H_{48}⋯O_{32}	1.86110	153.5	0.01348	-278.9
	O_{32}-H_{33}⋯O_{40}	1.91121	139.4	0.01459	-258.5
Epicat O_{32}-H_{33}⋯Ala O_{sp^3}	O_{32}-H_{33}⋯O_{47}	1.96248	168.9	0.0058	-114.5
	C_1-H_7⋯O_{47}	2.98091	125.1	-0.00098	11.2
Epicat O_{34}-H_{34}⋯Ala N_{sp^3}	O_{34}-H_{35}⋯N_{39}	1.84464	171.1	0.02576	-527.6
	C_{36}-H_{42}⋯O_{34}	2.80094	122.9	-0.00203	90.9
	C_5-H_8⋯N_{39}	2.98129	122.3	-0.00185	20.7
Epicat O_{34}-H_{34}⋯Ala O_{sp^2}	O_{34}-H_{35}⋯O_{40}	1.90422	176.6	0.009	-164.8
	C_5-H_8⋯O_{40}	2.72268	126.6	-0.00162	20.7
Epicat O_{34}-H_{34}⋯Ala O_{sp^3}	O_{34}-H_{35}⋯O_{47}	1.97709	171.3	0.00541	-107.3
	C_{36}-H_{41}⋯O_{34}	3.26338	133.9	-0.00274	110.5
	O_5-H_8⋯O_{47}	2.97008	125.0	-0.0009	12.4

Table 13. *Hybridization of the X atom of the X-H bond in monomers and in the X-H···Y contact and the variations of the S character of the X atom (ΔS%) with complexation for the Cat… Ala complex.*

Complexes	Hybridization sp^n (X-H)		Δ%S	$\Delta\sigma^*$ (10^{-3} e)	Complexes	Hybridization sp^n (X-H)		Δ%S	$\Delta\sigma^*$ (10^{-3} e)
	Monomers	Complexes				Monomers	Complexes		
$Cat\ O_{28}-H_{29}\cdots\ Ala\ N_{sp^3}$					$Cat\ O_{28}-H_{29}\cdots\ Ala\ O_{sp^2}$				
$LP_{N39}\rightarrow\sigma^*_{O28-H29}$	$sp^{3,40}$	$sp^{2,48}$	6	63.39	$LP_{O40}\rightarrow\sigma^*_{O28-H29}$	$sp^{3,40}$	$sp^{2,67}$	4.5	33.90
$LP_{O40}\rightarrow\sigma^*_{C22-H25}$	$sp^{2,37}$	$sp^{2,32}$	0.49	1.98	$LP_{O28}\rightarrow\sigma^*_{N39-H45}$	$sp^{2,93}$	$sp^{2,78}$	1.04	8.63
$LP_{O28}\rightarrow\sigma^*_{C36-H42}$	$sp^{3,04}$	$sp^{3,03}$	0.05	-0.08	$LP_{O40}\rightarrow\sigma^*_{C22-H25}$	$sp^{2,37}$	$sp^{2,34}$	0.27	0.27
$Cat\ O_{28}-H_{29}\cdots\ Ala\ O_{sp^3}$									
$LP_{O47}\rightarrow\sigma^*_{O28-H29}$	$sp^{3,40}$	$sp^{2,81}$	3.48	22.69					
$LP_{O28}\rightarrow\sigma^*_{N39-H46}$	$sp^{2,93}$	$sp^{2,78}$	1.04	5.46					
$LP_{O47}\rightarrow\sigma^*_{C22-H25}$	$sp^{2,37}$	$sp^{2,36}$	0.14	0.45					
$Cat\ O_{32}-H_{33}\cdots\ Ala\ N_{sp^3}$					$Cat\ O_{32}-H_{33}\cdots\ Ala\ O_{sp^2}$				
$LP_{N39}\rightarrow\sigma^*_{O32-H33}$	$sp^{3,53}$	$sp^{3,58}$	5.88	60.29	$LP_{O40}\rightarrow\sigma^*_{O32-H33}$	$sp^{3,53}$	$sp^{2,84}$	3.97	32.53
$LP_{N39}\rightarrow\sigma^*_{C1-H7}$	$sp^{2,24}$	$sp^{2,24}$	0.03	0.24	$LP_{O32}\rightarrow\sigma^*_{O47-H48}$	$sp^{3,45}$	$sp^{2,79}$	3.9	28.10
$Cat\ O_{32}-H_{33}\cdots\ Ala\ O_{sp^3}$									
$LP_{O47}\rightarrow\sigma^*_{O32-H33}$	$sp^{3,53}$	$sp^{2,98}$	3.09	19.67					
$LP_{O47}\rightarrow\sigma^*_{C1-H7}$	$sp^{2,24}$	$sp^{2,23}$	0.14	0.42					
$Cat\ O_{34}-H_{35}\cdots\ Ala\ N_{sp^3}$					$Cat\ O_{34}-H_{35}\cdots\ Ala\ O_{sp^2}$				
$LP_{N39}\rightarrow\sigma^*_{O34-H35}$	$sp^{3,56}$	$sp^{2,57}$	6.03	60.54	$LP_{O40}\rightarrow\sigma^*_{O34-H35}$	$sp^{3,56}$	$sp^{2,87}$	3.86	31.49
$LP_{O34}\rightarrow\sigma^*_{C36-H43}$	$sp^{3,14}$	$sp^{3,01}$	0.78	1.16	$LP_{O34}\rightarrow\sigma^*_{O47-H48}$	$sp^{3,45}$	$sp^{2,84}$	3.57	28.27
$LP_{N39}\rightarrow\sigma^*_{C5-H8}$	$sp^{2,28}$	$sp^{2,28}$	-0.03	0.29					
$Cat\ O_{34}-H_{35}\cdots\ Ala\ O_{sp^3}$									
$LP_{O47}\rightarrow\sigma^*_{O34-H35}$	$sp^{3,56}$	sp^{3}	3.02	18.23					
$LP_{O34}\rightarrow\sigma^*_{C37-H44}$	$sp^{3,13}$	$sp^{3,11}$	0.09	-0.29					
$LP^{(1)}_{O47}\rightarrow\sigma^*_{C5-H8}$	$sp^{2,28}$	$sp^{2,27}$	0.11	0.6					

3.4. Effect of Hybridization and "Hyperconjugative" Interactions

Tables 13 and 14 show the hybridization of the O_1 atom of the O_i-H_j hydroxyl groups of EpiCat and Cat. It also illustrates the variation of the s character of O_1 atoms. In the complexes EpiCat ⋯ Ala and Cat… Ala, there is the hybridization of the O_1 in the O_i-H_j⋯ O and O_i-H_j ⋯N. In monomers (EpiCat and Cat), O_1 atoms are hybridized sp^x (x ∈ 3.39 – 3.67) while in complexes, other oxygen are hybridized sp^m (m "∈" 2.48 – 3.58). There is a decrease in character p and an increase in s one (Δ%S > 0). The reduction in O_i-H_j bond length is a consequence of this second hybridization [46].

However, this work notes the presence of the "hyperconjugative" interactions $LP_O\rightarrow\sigma^*_{O_i\text{-}H_j}$ and $LP_N\rightarrow\sigma^*_{O_i\text{-}H_j}$ with high stabilization energies $E^{(2)}$; these vary from 7.45 kcal⁄mol to 31.54 kcal⁄mol. This interaction increases the electron density of the antibonding orbital $\sigma^*_{O_i-H_j}$ polarized along the HB axis. Thereby, it weakens the Oi – Hj bonds; it increases their length [46]. Its effects outweigh those of hybridization [39].

For HB C_i-H_j⋯O or C_i-H_j⋯N interactions, the carbon C is hybridized sp^x (x ∈ 2.23 - 3.15) whereas in Ala, EpiCat and Cat its homologs are hybridized sp^m (m ∈ 2.24 – 2.93), sp^n (n ∈ 3.04 – 3.14), sp^t (t ∈ 2.24 – 2.37) respectively. These values indicate that its hybridization increases its character s and lowers that of p. This hybridization contributes to contracting the C_i-H_j bond. In these complexes, "hyperconjugative" interactions result in $LP_O\rightarrow\sigma^*_{C_i\text{-}H_j}$ and $LP_N\rightarrow\sigma^*_{C_i\text{-}H_j}$; they correspond to low stabilization energies $E^{(2)}$; these go from 0.1 kcal⁄mol to 0.83 kcal⁄mol. This C_i-H_j bond shortening is illustrated in the data in tables 11 and 12. Its contraction ($\Delta d(C_i\text{-}H_j) < 0$) means that the effects of its hybridization outweigh those of "hyperconjugative" interactions.

Table 14. *X Hybridization in the X-H bond in monomers and in the X-H···Y contact and the variations of the s character of the X atom (ΔS%) with complexation for the Cat… Ala.*

	Hybridization sp^n (X-H)		Δ%S	$\Delta\sigma^*$ (10^{-3} e)	Complexes	Hybridization sp^n (X-H)		Δ%S	$\Delta\sigma^*$ (10^{-3} e)
	Monomers	Complexes				Monomers	Complexes		
$Epicat\ O_{28}-H_{29}\cdots\ Ala\ N_{sp^3}$					$Epicat\ O_{28}-H_{29}\cdots\ Ala\ O_{sp^2}$				
$LP_{N39}\rightarrow\sigma^*_{O28-H29}$	$sp^{3,39}$	$sp^{2,48}$	6	66.62	$LP_{O40}\rightarrow\sigma^*_{O28-H29}$	$sp^{3,39}$	$sp^{2,66}$	4.54	34.56
$LP_{O28}\rightarrow\sigma^*_{C36-H42}$	$sp^{3,04}$	$sp^{3,05}$	-0.06	-0.22	$LP_{O28}\rightarrow\sigma^*_{N46-H48}$	$sp^{2,93}$	$sp^{2,78}$	1.01	8.40
					$LP_{O40}\rightarrow\sigma^*_{C22-H25}$	$sp^{2,32}$	$sp^{2,35}$	-0.21	0.97
$Epicat\ O_{28}-H_{29}\cdots\ Ala\ O_{sp^3}$									
$LP_{O47}\rightarrow\sigma^*_{O28-H29}$	$sp^{3,39}$	$sp^{2,84}$	3.26	20.76					
$LP_{O28}\rightarrow\sigma^*_{C36-H41}$	$sp^{3,04}$	$sp^{3,01}$	-	-0.52					

	Hybridization sp^n (X-H)		Δ%S	$\Delta\sigma^*$ (10^{-3} e)	Complexes	Hybridization sp^n (X-H)		Δ%S	$\Delta\sigma^*$ (10^{-3} e)
	Monomers	Complexes				Monomers	Complexes		
			0.12						
$LP_{O47} \rightarrow \sigma^*_{C22-H25}$	$sp^{2,32}$	$sp^{2,37}$	-0.44	1.35					
Epicat $O_{32} - H_{33} \cdots$ Ala N_{sp^3}					Epicat $O_{32} - H_{33} \cdots$ Ala O_{sp^2}				
$LP_{N39} \rightarrow \sigma^*_{O32-H33}$	$sp^{3,56}$	$sp^{2,58}$	5.95	59.72	$LP_{O32} \rightarrow \sigma^*_{O47-H48}$	$sp^{3,45}$	$sp^{2,84}$	3.55	28.32
$LP_{N39} \rightarrow \sigma^*_{C1-H7}$	$sp^{2,28}$	$sp^{2,24}$	0.38	-0.63	$LP_{O40} \rightarrow \sigma^*_{O32-H33}$	$sp^{3,56}$	$sp^{2,86}$	3.98	31.15
Epicat $O_{32} - H_{33} \cdots$ Ala O_{sp^3}									
$LP_{O47} \rightarrow \sigma^*_{O32-H33}$	$sp^{3,56}$	$sp^{2,97}$	3.21	19.20					
$LP_{O32} \rightarrow \sigma^*_{C37-H44}$	$sp^{3,13}$	$sp^{3,15}$	-0.12	-2.45					
Epicat $O_{34} - H_{35} \cdots$ Ala N_{sp^3}					Epicat $O_{34} - H_{35} \cdots$ Ala O_{sp^2}				
$LP_{N43} \rightarrow \sigma^*_{O34-H35}$	$sp^{3,67}$	$sp^{2,61}$	6.24	59.60	$LP_{O40} \rightarrow \sigma^*_{O34-H35}$	$sp^{3,67}$	$sp^{2,93}$	3.99	32.79
$LP_{O34} \rightarrow \sigma^*_{C36-H41}$	$sp^{3,04}$	$sp^{3,02}$	0.12	-0.13	$LP_{O40} \rightarrow \sigma^*_{C5-H8}$	$sp^{2,24}$	$sp^{2,23}$	0.07	1.84
$LP_{N43} \rightarrow \sigma^*_{C5-H8}$	$sp^{2,24}$	$sp^{2,28}$	-0.38	1.02					
Epicat $O_{34} - H_{35} \cdots$ Ala O_{sp^3}									
$LP_{O47} \rightarrow \sigma^*_{O34-H35}$	$sp^{3,67}$	$sp^{3,02}$	3.45	19.28					
$LP_{O34} \rightarrow \sigma^*_{C36-H41}$	$sp^{3,04}$	$sp^{3,02}$	0.09	-1.19					
$LP_{O47} \rightarrow \sigma^*_{C5-H8}$	$sp^{2,24}$	$sp^{2,26}$	-0.21	1.29					

3.5. AIM Analysis

Figures 6 and 7 illustrate, as an example, the AIM-molecular graphs of Epicat $O_{28} - H_{29} \cdots$ Ala N_{sp^3}, Epicat $O_{28} - H_{29} \cdots$ Ala O_{sp^2} and Epicat $O_{28} - H_{29} \cdots$ Ala O_{sp^3} and then Cat $O_{28} - H_{29} \cdots$ Ala N_{sp^3}, Cat $O_{28} - H_{29} \cdots$ Ala O_{sp^2} and Cat $O_{28} - H_{29} \cdots$ Ala O_{sp^3} complexes, respectively; the small green spheres are BCP.

Tables 15 and 16 present results of the X-H···Y BCP (X=O, N, C) and (Y=O, N) interactions topological analyzes for EpiCat ··· Ala and Cat ··· Ala complexes. In these, the electronic density ρ(r) between the hydroxyl groups $O_I - H_j$ with the Nsp^3, Osp^2 and Osp^3 heteroatoms of Ala, vary between 0.004408 ea_0^{-3} and 0.043552 ea_0^{-3}. Those of $\nabla 2$ ρ(r) range from 0.017568 ea_0^{-5} to 0.101413 ea_0^{-5}. Values of $\nabla 2$ ρ(r) are positive. They indicate that these interactions are HB. Their total negative electron energy density H(r) O_i-$H_j \cdots N_{sp^3}$, O_i-$H_j \cdots O_{sp^2}$ and O_i-$H_j \cdots O_{sp^3}$ reflects moderate HB [40]. Moreover, this work adopts ratios $-\frac{G(r)}{V(r)}$ between 0.5 and 1. These moderate HB are partially covalent.

The total electron energy density H(r) is slightly positive for the interactions O_{34}-$H_{35} \cdots O_{40}$, O_{28}-$H_{29} \cdots O_{40}$ of EpiCat ··· Ala complexes and O_{28}-$H_{29} \cdots O_{40}$, O_{28}-$H_{29} \cdots O_{47}$ for those formed from Cat ···Ala Their $-\frac{G(r)}{V(r)}$ ratios are greater than 1. These values correspond to interactions which are within the moderate HB limit with a partially covalent character. Those of the HB E_{HB} energies calculated using Espinoza's method are reported in the last columns of tables 15 and 16. For the interactions linked to hydroxyl groups $O_I - H_j$, they vary from 5.0929938 kcal⁄mol to 10.0687117 kcal⁄mol. These interactions are moderate HB; they meet Espinoza's criteria (4 kcal⁄mole < E_{HB} < 15 kcal⁄mole) [51]. They include the interactions O_{32}-$H_{33} \cdots N_{39}$(E_{HB}= 8.80 kcal⁄mol), O_{32}-$H_{33} \cdots O_{40}$ (E_{HB}= 7.22 kcal⁄mol), O_{32}-$H_{33} \cdots O_{47}$ (E_{HB}= 4.60 kcal⁄mol), O_{34}-$H_{35} \cdots N_{39}$ (E_{HB}= 8.35 kcal⁄mol), O_{34}-$H_{35} \cdots O_{40}$ (E_{HB}= 7.14 kcal⁄mol), O_{34}-$H_{35} \cdots O_{47}$ (E_{HB}= 5.27 kcal⁄mol), O_{28}-$H_{29} \cdots N_{39}$ (E_{HB}= 8.71 kcal⁄mol), O_{28}-$H_{29} \cdots O_{40}$ (E_{HB}= 7.47 kcal⁄mol) et O_{28}-$H_{29} \cdots O_{47}$ (E_{HB}= 6.08 kcal/mol) of Cat ··· Ala complexes (Table 15). For the EpiCat… Ala ones (Table 16), they are the O_{32}-$H_{33} \cdots N_{39}$ (E_{HB} = 8.69 kcal/mol), O_{32}-$H_{33} \cdots O_{40}$ (E_{HB} = 7.05 kcal/mol), O_{32}-$H_{33} \cdots O_{47}$ (E_{HB}= 5.44 kcal⁄mol), O_{34}-$H_{35} \cdots N_{39}$ (E_{HB}= 8.05 kcal/mol), O_{34}-$H_{35} \cdots O_{40}$ (E_{HB}= 5.71 kcal/mol), O_{34}-$H_{35} \cdots O_{47}$ (E_{HB}= 5.29 kcal⁄mol), O_{28}-$H_{29} \cdots N_{39}$ (E_{HB}= 9.16 kcal⁄mol), O_{28}-$H_{29} \cdots O_{40}$ (E_{HB}= 7.55 kcal⁄mol), O_{28}-$H_{29} \cdots O_{47}$ (E_{HB}= 5.62 kcal⁄mol. However, for C-H···O and N-H···O interactions, the values of $\nabla 2$ ρ (r) and H(r) are positive. Those of C-H···O and N-H···O are weak. Moreover, the $-\frac{G(r)}{V(r)}$ ratios are greater than 1. They suggest that their characters be non-covalent or electrostatic. E_{HB} values are less than 4 kcal⁄mol.

Table 15. *AIM parameters of BCP of Cat ···Ala interactions.*

Contact	$\rho(r)_{X-H\cdots Y}$ $\left(ea_0^{-3}\right)$	$\nabla^2\rho(r)_{X-H\cdots Y}$ $\left(ea_0^{-5}\right)$	V(r) (ua)	G(r) (ua)	H(r) (ua)	$-\frac{G(r)}{V(r)}$	E_{HB} (kcal/mole)
Cat O_{28}-$H_{29} \cdots$ Ala N_{sp^3}							
O_{28}-$H_{29} \cdots N_{39}$	0.04182	0.090873	-0.027754	0.025236	-0.002518	0.91	8.71
C_{22}-$H_{25} \cdots O_{40}$	0.006168	0.021917	-0.003838	0.004658	0.00082	1.21	1.20
Cat O_{28}-$H_{29} \cdots$ Ala O_{sp^2}							
O_{28}-$H_{29} \cdots O_{40}$	0.032491	0.100229	-0.023805	0.024431	0.000626	1.03	7.47

Contact	$\rho(r)_{X-H\cdots Y}\left(ea_0^{-3}\right)$	$\nabla^2\rho(r)_{X-H\cdots Y}\left(ea_0^{-5}\right)$	V(r) (ua)	G(r) (ua)	H(r) (ua)	$-\frac{G(r)}{V(r)}$	$E_{HB}\left(kcal/mole\right)$
N_{39}-$H_{45}\cdots O_{28}$	0.011022	0.036611	-0.008111	0.008632	0.000521	1.06	2.54
Cat O_{28}-$H_{29}\cdots$ Ala O_{sp^3}							
O_{28}-$H_{29}\cdots O_{47}$	0.025778	0.078407	-0.019391	0.019496	0.000105	1.01	6.08
N_{39}-$H_{46}\cdots O_{28}$	0.011117	0.035634	-0.008101	0.008505	0.000404	1.05	2.54
Cat O_{32}-$H_{33}\cdots$ Ala N_{sp^3}							
O_{32}-$H_{33}\cdots N_{39}$	0.041844	0.092378	-0.028034	0.025564	-0.00247	0.91	8.80
Cat O_{32}-$H_{33}\cdots$ Ala O_{sp^2}							
O_{32}-$H_{33}\cdots O_{40}$	0.02975	0.085458	-0.023009	0.022187	-0.000822	0.96	7.22
O_{47}-$H_{48}\cdots O_{32}$	0.030158	0.088992	-0.022603	0.022425	-0.000178	0.99	7.09
Cat O_{32}-$H_{33}\cdots$ Ala O_{sp^3}							
O_{32}-$H_{33}\cdots O_{47}$	0.018988	0.057703	-0.014663	0.014544	-0.000119	0.99	4.60
C_1-$H_7\cdots O_{47}$	0.006556	0.022644	-0.004028	0.004844	0.000816	1.20	1.26
Cat O_{34}-$H_{35}\cdots$ Ala N_{sp^3}							
O_{34}-$H_{35}\cdots N_{39}$	0.040465	0.089222	-0.026609	0.024457	-0.002152	0.92	8.35
Cat O_{34}-$H_{35}\cdots$ Ala O_{sp^2}							
O_{34}-$H_{35}\cdots O_{40}$	0.029382	0.084394	-0.02275	0.021924	-0.000826	0.96	7.14
O_{47}-$H_{48}\cdots O_{34}$	0.029843	0.087166	-0.022276	0.022034	-0.000242	0.99	6.99
Cat O_{34}-$H_{35}\cdots$ Ala O_{sp^3}							
O_{34}-$H_{35}\cdots O_{47}$	0.022293	0.066072	-0.016785	0.016651	-0.000134	0.99	5.27
C_{36}-$H_{41}\cdots H_8$-C_5	0.001478	0.004523	-0.000526	0.000829	0.000303	1.58	0.17

Table 16. *AIM parameters of the bond critical point (BCP) of EpiCat ⋯ Ala interactions.*

Contact	$\rho(r)_{X-H\cdots Y}\left(ea_0^{-3}\right)$	$\nabla^2\rho(r)_{X-H\cdots Y}\left(ea_0^{-5}\right)$	V(r) (ua)	G(r) (ua)	H(r) (ua)	$-\frac{G(r)}{V(r)}$	$E_{HB}\left(kcal/mole\right)$
Epicat O_{28}-$H_{29}\cdots$ Ala N_{sp^3}							
O_{28}-$H_{29}\cdots N_{39}$	0.043552	0.093384	-0.029193	0.02627	-0.002923	0.900	9.16
Epicat O_{28}-$H_{29}\cdots$ Ala O_{sp^2}							
O_{28}-$H_{29}\cdots O_{40}$	0.032866	0.101413	-0.024061	0.024707	0.000646	1.027	7.55
N_{39}-$H_{46}\cdots O_{28}$	0.010796	0.036099	-0.007924	0.008474	0.000550	1.069	2.49
Epicat O_{28}-$H_{29}\cdots$ Ala O_{sp^3}							
O_{28}-$H_{29}\cdots O_{47}$	0.024023	0.072554	-0.017924	0.018031	0.000107	1.006	5.62
C_{36}-$H_{41}\cdots O_{28}$	0.004408	0.017568	-0.002366	0.003379	0.001013	1.428	0.74
Epicat O_{32}-$H_{33}\cdots$ Ala N_{sp^3}							
O_{32}-$H_{33}\cdots N_{39}$	0.041471	0.091515	-0.027694	0.025286	-0.002408	0.913	8.69
Epicat O_{32}-$H_{33}\cdots$ Ala O_{sp^2}							
O_{47}-$H_{48}\cdots O_{32}$	0.030009	0.087435	-0.022426	0.022142	-0.000284	0.987	7.04
O_{32}-$H_{33}\cdots O_{40}$	0.029005	0.083394	-0.02248	0.021664	-0.000816	0.964	7.05
Epicat O_{32}-$H_{33}\cdots$ Ala O_{sp^3}							
O_{32}-$H_{33}\cdots O_{47}$	0.022996	0.068124	-0.017323	0.017177	-0.000146	0.992	5.44
C_{36}-$H_{41}\cdots H_7$-C_1	0.001642	0.005001	-0.000593	0.000922	0.000329	1.555	0.19
Epicat O_{34}-$H_{35}\cdots$ Ala N_{sp^3}							
O_{34}-$H_{35}\cdots N_{39}$	0.039207	0.086047	-0.025642	0.023577	-0.002065	0.919	8.05
Epicat O_{34}-$H_{35}\cdots$ Ala O_{sp^2}							
O_{34}-$H_{35}\cdots O_{40}$	0.024635	0.078477	-0.018194	0.018906	0.000712	1.039	5.71
C_5-$H_8\cdots O_{40}$	0.006104	0.022354	-0.003629	0.004609	0.000980	1.270	1.14
N_{39}-$H_{45}\cdots C_5 = C_6$	0.005379	0.017954	-0.002411	0.00345	0.001039	1.431	0.76
Epicat O_{34}-$H_{35}\cdots$ Ala O_{sp^3}							
O_{34}-$H_{35}\cdots O_{47}$	0.02241	0.065291	-0.016853	0.016588	-0.000265	0.984	5.29
C_{36}-$H_{41}\cdots H_8$-C_5	0.001906	0.006106	-0.000723	0.001125	0.000402	1.556	0.23

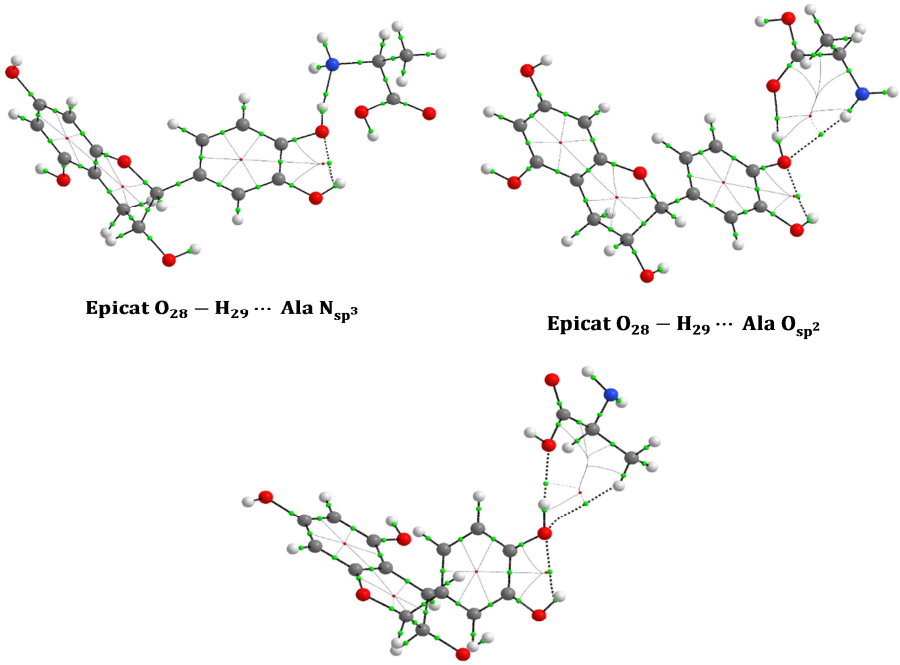

Figure 6. *AIM molecular plots of the Cat O_{28}-$H_{29}\cdots$Ala N_{sp^3} Cat O_{28}-$H_{29}\cdots$Ala O_{sp^2} and Cat O_{28}-$H_{29}\cdots$Ala O_{sp^3}.*

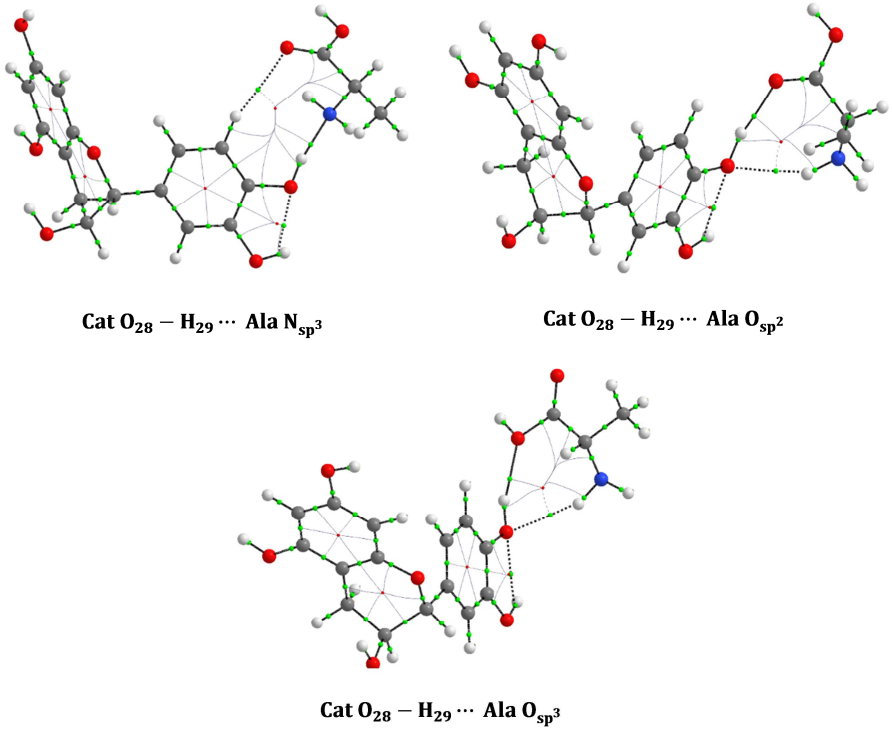

Figure 7. *AIM molecular plots of the Epicat O_{28}-$H_{29}\cdots$Ala N_{sp^3} Epicat O_{28}-$H_{29}\cdots$Ala O_{sp^2} and Epicat O_{28}-$H_{29}\cdots$Ala O_{sp^3} complexes.*

3.6. NCI Analysis

The NCI analysis is restricted to the interactions of the O_{28} – H_{29} hydroxyl group of EpiCat and Cat with the N_{sp^3}, O_{sp^2} and O_{sp^3} heteroatoms of Ala These are the Epicat O_{28}-$H_{29}\cdots$Ala N_{sp^3} , Epicat O_{28}-$H_{29}\cdots$Ala O_{sp^2} , Epicat O_{28}-$H_{29}\cdots$Ala O_{sp^3} , Cat O_{28}-$H_{29}\cdots$Ala N_{sp^3} , Cat O_{28}-$H_{29}\cdots$Ala O_{sp^2} and Cat O_{28}-$H_{29}\cdots$Ala O_{sp^3}. Figure 8 shows the NCI iso-surfaces and RDG (Reduced Density Gradient) plots as a function of (sign λ_2) × ρ of the EpiCat… Ala and Cat… Ala complexes.

In Epicat O_{28}-$H_{29}\cdots$Ala N_{sp^3} and Cat O_{28}-$H_{29}\cdots$Ala N_{sp^3} complexes, NCI analysis suggests the presence of HB and repulsive interaction. The bonds O-H ⋯ N, O-H ⋯ O and C-

H ⋯ O are revealed by peak appearance at - 0.040 a.u < (sign λ_2) × ρ < - 0.010 a.u while the repulsive interactions O ⋯ O, H ⋯ H, C ⋯ C have their peaks appearing at 0.010 a.u < (sign λ_2) × ρ < 0.020 a.u. The blue "NCI" between the H and N; H and O atoms characterize the presence of the previously mentioned O-H ⋯ N, O-H ⋯ O and C-H ⋯ O HB. Similarly, the red-coloured "isosurfaces" between O and O; C and C and within the rings are associated with the existence of repulsive interactions.

For complexes Epicat O_{28}-H_{29}⋯Ala O_{sp^2}, Epicat O_{28}-H_{29}⋯Ala O_{sp^3}, Cat O_{28}-H_{29}⋯Ala O_{sp^2} and Cat O_{28}-H_{29}⋯Ala O_{sp^3}, research notes that VDW interactions overlap with HB and repulsive ones; the presence of peaks at (sign λ 2) × ρ = 0 attests to this. Moreover, the green-coloured "isosurface" between the hydrogen H atoms reinforces this hypothesis.

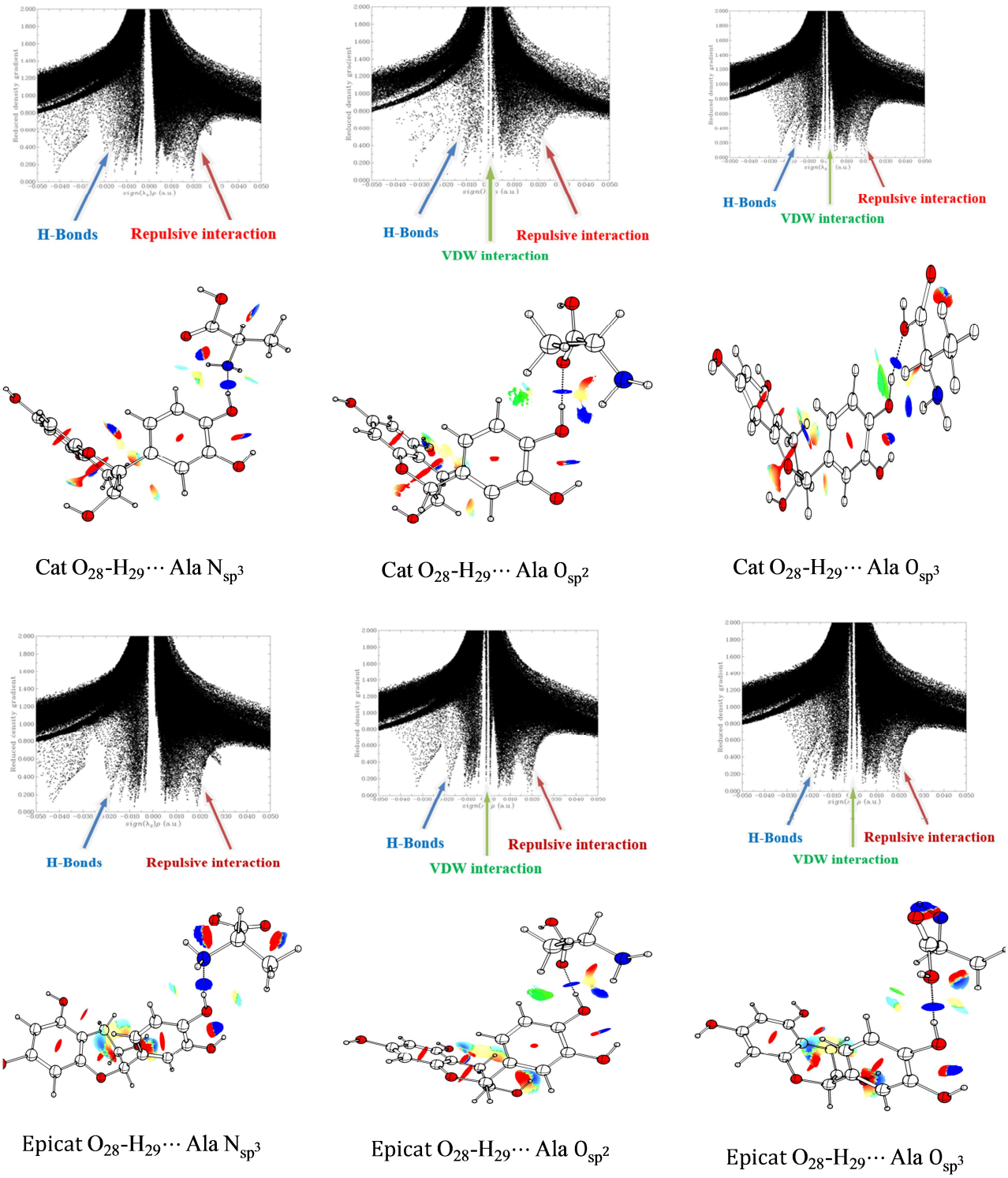

Figure 8. *NCI "isosurface" and gradients plot of the RDG as a function of* (signλ_2)×ρ *of some Cat… Ala and EpiCat… Ala complexes.*

4. Conclusion

This study focused on the interactions between EpiCat and Ala and between Cat and Ala. According to the optimized geometries of the EpiCat… Ala and Cat complexes… Ala formed, the energies, vibrational frequencies, CT, and topological parameters were analyzed. It aims to identify the nature and category of interactions in the EpiCat… Ala and Cat… Ala complexes. It intends to specify whether they are covalently based on quantitative data. Following the optimization of their geometries, it focuses on the energetic and vibrational aspects associated with these two complexes. It evaluates CT within them and their topological parameters. Right off the bat, the assessment of this data makes it possible to discuss their stability. The enthalpies of formation and free Gibbs enthalpies show that the synthesis of EpiCat… Ala and Cat… Ala is exothermic and spontaneous in the gas phase. Afterwards, NBO analysis reveals the presence of several non-covalent interactions including O – H···O, O – H···N, C – H···O, C – H···N, N – H···O, O – H···π, C - H ··· π, N - H ··· π. Furthermore, this work establishes that O - H ··· O and O - H ··· N are the main ones; these possess the highest stabilization energies. Moreover, examination of the complexes vibrational frequencies suggests that O - H···O, O - H···N and N - H···O are appropriate or conventional HB. It proves that C - H ··· O and C - H ··· N are inappropriate or unconventional HB. In addition, this work is based on the parameters obtained at the various BCP and on the AIM analysis results to categorize these latter of the EpiCat… Ala and Cat… Ala complexes to classify the HB. It demonstrates that O – H···O and O – H···N are weak and partially covalent whereas C – H···O, C – H···N and N – H···O are also feeble and non-covalent. Finally, the study of the stabilization energies $E^{(2)}$, of the CT and of the E_{HB} establishes that the most active sites are the hydroxyl groups $O_{28} - H_{29}$, $O_{32} - H_{33}$ and $O_{34} - H_{35}$ for EpiCat and Cat and the N_{sp^3} and O_{sp^2} heteroatoms of Ala These sites lead to the most stable complexes.

References

[1] Jian Zhao, Lawrence Davis and Robert Verpoorte. (2005). Elicitor signal transduction leading to production of plant secondary metabolites. *Biotechnology advances.* (4). doi: 10.1016/j.biotechadv.2005.01.003.

[2] María Lorena Falcone Ferreyra, Sebastián Pablo Rius and Paula Casati. (2012). Flavonoids: Biosynthesis, biological functions, and biotechnological applications. *Frontiers in plant science*. doi: 10.3389/fpls.2012.00222.

[3] Victor Preedy. (2012). Tea in Health and Disease Prevention, Elsevier Science and Technology Books, San Diego, CA, USA.

[4] Debora Villaño, Maria Soledad Fernández-Pachón, Maria Luisa Moyá, Ana Troncoso and Maria del Carmen Garcia-Parilla. (2007). Radical scavenging ability of polyphenolic compounds towards DPPH free radical. *Talanta.* (1). doi: 10.1016/j.talanta.2006.03.050.

[5] Marta González-Castejón and Arantxa Rodriguez-Casado. (2011). Dietary phytochemicals and their potential effects on obesity: A review. *Pharmacological research.* (5). doi: 10.1016/j.phrs.2011.07.004.

[6] Narumi Sugihara, Mikae Ohnishi, Masahiro Imamura et al. (2001). Differences in Antioxidative Efficiency of Cat in Various Metal-Induced Lipid Peroxidations in Cultured Hepatocytes. *Journal of HEALTH SCIENCE.* (2). doi: 10.1248/jhs.47.99.

[7] Liting Zhao, Jianquan Wu, Yuping Wang, Jijun Yang, Jingyu Wei … and Weina Gao. (2011). Cholesterol metabolism is modulated by quercetin in rats. *Journal of agricultural and food chemistry.* (4). doi: 10.1021/jf1035367.

[8] Francesca Oliviero, Anna Scanu, Yessica Zamudio-Cuevas, Leonardo Punzi and Paolo Spinella. (2018). Anti-inflammatory effects of polyphenols in arthritis. *Journal of the science of food and agriculture.* (5). doi: 10.1002/jsfa.8664.

[9] Peter Hollman, Aedin Cassidy, Blandine Comte, Marina Heinonen, Myriam Richelle … and Stephane Vidry. (2011). The biological relevance of direct antioxidant effects of polyphenols for cardiovascular health in humans is not established. *The Journal of nutrition.* (5). doi: 10.3945/jn.110.131490.

[10] Claudine Manach, Andrzej Mazur and Augustin Scalbert. (2005). Polyphenols and prevention of cardiovascular diseases. *Current opinion in lipidology.* (1). doi: 10.1097/00041433-200502000-00013.

[11] Alan Crozier, Indu Jaganath and Michael Clifford. (2009). Dietary phenolics: Chemistry, bioavailability and effects on health. *Natural product reports.* (8). doi: 10.1039/B802662A.

[12] Elham Assadpour. (2017). Protection of phenolic compounds within nanocarriers. *CAB Reviews: Perspectives in Agriculture, Veterinary Science, Nutrition and Natural Resources.* (57). doi: 10.1079/PAVSNNR201712057.

[13] Jonathan Hart, Elad Tako, Leon Kochian and Raymond Glan. (2015). Identification of Black Bean (Phaseolus vulgaris L.) Polyphenols That Inhibit and Promote Iron Uptake by Caco-2 Cells. *Journal of agricultural and food chemistry.* (25). doi: 10.1021/acs.jafc.5b00531.

[14] Satoshi Uchiyama, Yoshimasa Taniguchi, Akiko Saka, Aruto Yoshida and Hiroaki Yajima. (2011). Prevention of diet-induced obesity by dietary black tea polyphenols extracts in vitro and in vivo. *Nutrition (Burbank, Los Angeles County, Calif.).* (3). doi: 10.1016/j.nut.2010.01.019.

[15] Carine Le Bourvellec, Sylvain Guyot and Catherine Marie Genevieve Claire Renard. (2004). Non-covalent interaction between procyanidins and apple cell wall material: Part I. The effect of some environmental parameters. *Biochimica et biophysica acta.* (3). doi: 10.1016/j.bbagen.2004.04.001.

[16] Prasun Bandyopadhyay, Amit Kumar Ghosh and Chandrasekhar Ghosh. (2012). Recent developments on polyphenols—protein interactions: Effects on tea and coffee taste, antioxidant properties and the digestive system. *Food and function.* (6). doi: 10.1039/C2FO00006G.

[17] Elisabeth Jöbstl, John O'Connell, Patrick Fairclough and Mike Williamson. (2004). Molecular model for astringency produced by polyphenol/protein interactions. *Biomacromolecules.* (3). doi: 10.1021/bm0345110.

[18] Mourad Elhabiri, Charlotte Carrer, Franck Marmolle and Hassan Traboulsi. (2007). Complexation of iron (III) by catecholate-type polyphenols. *Inorganica Chimica Acta.*(1). doi: 10.1016/j.ica.2006.07.110.

[19] Akpa Eugene Essoh, Boka Robert N'guessan, Ganiyou Adenidji, Kicho Denis Yapo, Ane Adjou and El Hadji Sawaliho Bamba. (2022). Catechin and Epicatechin. What's the More Reactive? *Computational Chemistry.* (02). doi: 10.4236/cc.2022.102003.

[20] Karl Siebert, Nataliia Troukhanova and Penelope Lynn. (1996). Nature of Polyphenol−Protein Interactions. *Journal of Agricultural and Food Chemistry.* (1). doi: 10.1021/jf9502459.

[21] Cecile Simon, Karine Barathieu, Michel Laguerre, Jean-Marie Schmitter, Eric Fouquet … and Eric Dufourc. (2003). Three-dimensional structure and dynamics of wine tannin-saliva protein complexes. A multitechnique approach. *Biochemistry.* (35). doi: 10.1021/bi034354p.

[22] Zerrin Yuksel, Elif Avci and Yasar Kemal Erdem. (2010). Characterization of binding interactions between green tea flavonoids and milk proteins. *Food Chemistry.* (2). doi: 10.1016/j.foodchem.2009.12.064.

[23] Jinfeng Liu, Xiao He, John Zhang and Lian-wen Qi. (2018). Hydrogen-bond structure dynamics in bulk water: Insights from ab initio simulations with coupled cluster theory. *Chemical science.* (8). doi: 10.1039/C7SC04205A.

[24] Harshadrai Rawel, Dörte Czajka, Sascha Rohn and Jürgen kroll. (2002). Interactions of different phenolic acids and flavonoids with soy proteins. *International Journal of Biological Macromolecules.* (3–4). doi: 10.1016/s0141-8130 (02)00016-8.

[25] Jürgen Kroll, Harshadrai Rawel and Sascha Rohn. (2003). Reactions of Plant Phenolic with Food Proteins and Enzymes under Special Consideration of Covalent Bonds. *Food Science and Technology Research.* (3). doi: 10.3136/fstr.9.205.

[26] Augustin Scalbert, Claudine Manach, Christine Morand, Christian Remesy and Liliana Jimenez. (2005). Dietary polyphenols and the prevention of diseases. *Critical reviews in food science and nutrition.* (4). doi: 10.1080/1040869059096.

[27] Judith Mak. (2012). Potential role of green tea catechin in various disease therapies: Progress and promise. *Clinical and experimental pharmacology and physiology.* (3). doi: 10.1111/j.1440-1681.2012.05673.x.

[28] Rahul Lall, Deeba Syed, Vaqar Adhami, Mohammad Imran Khan and Hasan Mukhtar. (2015). Dietary polyphenols in the prevention and treatment of prostate cancer. *International journal of molecular sciences.* (2). doi: 10.3390/ijms16023350.

[29] Robert Ghormley Parr. (1980). Density Functional Theory of Atoms and Molecules. Horizons of Quantum Chemistry. International Academy of Quantum Molecular Science. (3). doi.org/10.1007/978-94-009-9027-2_2.

[30] Michael Frisch, G. W. Trucks, H. B. Schlegel, G. E. Scuseria, M. A. Robb … and D. J. Fox. (2009), Gaussian 09 Revision D.01. Gaussian, Inc., Wallingford, CT,

[31] Todd Keith. (2010). AIMAll. 10.05.04.

[32] Eric D. Glendening, A. E. Reed and J. E. Carpenter. (2003). NBO. 3.1.

[33] G. A. Zhurko, D. A. Zhurko. Chemcraft. Version 1.8 (Build 523a).

[34] Tian Lu and Feiwu Chen. (2012). Multiwfn: a multifunctional wavefunction analyzer. *Journal of computational chemistry.* (5). doi: 10.1002/jcc.22885.

[35] Samuel Francis Boys and Fabriozo. Bernardi. (2006). The calculation of small molecular interactions by the differences of separate total energies. Some procedures with reduced errors. *Molecular Physics.* (4). doi: 10.1080/00268977000101561.

[36] Natarajan Sathiyamoorthy Venkataramanan and Ambigapathy Suvitha. (2017). Structure, electronic, inclusion complex formation behaviour and spectral properties of pillarplex. *Journal of Inclusion Phenomena and Macrocyclic Chemistry.* (1–2). doi: 10.1007/s10847-017-0711-y.

[37] M. Snehalatha, C. Ravikumar, I. Hubert Joe, N. Sekar and V. S. Jayakumar (2009). Spectroscopic analysis and DFT calculations of a food additive carmoisine. *Spectrochimica acta. Part A, Molecular and biomolecular spectroscopy.* (3). doi: 10.1016/j.saa.2008.11.017.

[38] Alan Reed, Larry Curtiss and Frank Weinhold. (1988). Intermolecular interactions from a natural bond orbital, donor-acceptor viewpoint. *Chemical Reviews.* (6). doi: 10.1021/cr00088a005.

[39] Richard Frederick William Bader. (1994). Atoms in molecules: A quantum theory, Clarendon Press; Oxford University press, Oxford, England, New York.

[40] Marcin Ziółkowski, Sławomir Grabowski and Jerzy Leszczynski. (2006). Cooperativeness in hydrogen-bonded interactions: ab initio and "atoms in molecules" analyses. *The journal of physical chemistry. A.*(20). doi: 10.1021/jp060537k.

[41] Isabel Rozas, Ibon Alkorta and Jose Elguero. (2000). Behaviour of Ylides Containing N, O, and C Atoms as Hydrogen Bond Acceptors. *Journal of the American Chemical Society.* (45). doi: 10.1021/ja0017864.

[42] Enrique Espinosa, Elies Molins and Claude Lecomte. (1998). Hydrogen bond strengths revealed by topological analyses of experimentally observed electron density. *Chemical Physics Letters.* (3–4). doi: 10.1016/S0009-2614 (98)00036-0.

[43] Natarajan Sathiyamoorthy Venkataramanan, Ambigapathy Suvitha and Yoshiyuki Kawazoe. (2017). Intermolecular interaction in nucleobases and dimethyl sulphoxide/water molecules: A DFT, NBO, AIM and NCI analysis. *Journal of molecular graphics and modelling.* doi: 10.1016/j.jmgm.2017.09.022.

[44] Natarajan Sathiyamoorthy Venkataramanan and Ambigapathy Suvitha. (2018). Nature of bonding and cooperativeness in linear DMSO clusters: A DFT, AIM and NCI analysis. *Journal of Molecular Graphics and Modelling.* doi: 10.1016/j.jmgm.2018.02.010.

[45] Debdutta Chakraborty and Pratim Kumar Chattaraj. (2018). Confinement induced thermodynamic and kinetic facilitation of some Diels-Alder reactions inside a CB7 cavitand. *Journal of computational chemistry.* (3). doi: 10.1002/jcc.25094.

[46] Igor Alabugin, Mariappan Manoharan, Scott Peabody and Frank Weinhold. (2003). Electronic basis of improper hydrogen bonding: A subtle balance of hyperconjugation and re-hybridization. *Journal of the American Chemical Society.* (19). doi: 10.1021/ja034656e.

[47] Ponmalai Kolandaivel and V. Nirmala. (2004). Study of proper and improper hydrogen bonding using Bader's atoms in molecules (AIM) theory and NBO analysis. *Journal of Molecular Structure.* (1–3). doi: 10.1016/j.molstruc.2004.01.030.

[48] Pavel Hobza and Zdenek Havlas. (2000). Blue-Shifting Hydrogen Bonds. *Chemical reviews.* (11). doi: 10.1021/cr990050q.

[49] Elangannan Arunan, Gautam Desiraju, Roger Klein, Joanna Sadlej, Steve Scheiner … and David Nesbitt. (2011). Definition of the hydrogen bond (IUPAC Recommendations 2011). *Pure and Applied Chemistry.* (8). doi: 10.1351/pac-rec-10-01-02.

[50] Mylsamy Karthika, Ramasamy Kanakaraju and Lakshmipathi Senthilkumar. (2013). Spectroscopic investigations and hydrogen bond interactions of 8-Aza analogues of xanthine, theophylline and caffeine: A theoretical study. *Journal of molecular modelling.* (4). doi: 10.1007/s00894-012-1742-3.

[51] Gautam Desiraju and Thomas Steiner. (1999). The weak hydrogen bond: In structural chemistry and biology, Oxford University press, Oxford, etc.